POLITECNICO DI TORINO

Master's Degree in Mechanical engineering

Master's Degree Thesis

"Algorithm for estimating the sideslip angle of a vehicle"

Supervisor
Prof. Enrico Galvagno
Prof. Alessandro Vigliani

Candidate
Antonino Napolitano

Academic Year 2020/2021

To my family.

Acknowledgments

All the activity was carried out in a difficult historical period. Despite the problems due to the unexpected worldwide pandemic, the DIMEAS research group gave me the opportunity to undertake this work in collaboration with the Stellantis Group.

For this reason, I want to thank prof. Galvagno and prof. Vigliani for the opportunity and their technical support throughout the thesis period and for helping me to grow from a technical and personal point of view.

I am grateful to Stellantis engineers who followed me during this period and in particular I thank Eng. Roberto Cunego who daily followed me, always providing me with new ideas and ways to improve myself, Eng. Alessandro Peyrot who provided me with great support in initially approaching this project, and Eng. Matteo Eugenio Sacchi who helped me to grow from professional point of view.

Finally, I want to thank all the people who have been close to me during this period by providing me with support in times of difficulty.

Abstract

The objective of this thesis is to generate a model that estimates the sideslip angle of a vehicle and, more generally, evaluates different parameters of the car for different types of tests. The model is based on the use of a linear Kalman filter. The input data to the model were obtained from the acquisition of both the CAN network and the IMU Inertial platform. The model has been validated for different types of cars with different tyres, rims and suspension types. Furthermore, the estimation of the model must take place quickly, therefore the model must have a computational cost as low as possible but also provide a good estimate of the parameters involved.
In the first part of the thesis the general theory of vehicle dynamics themes was treated with particular attention to lateral dynamics. In particular, the bicycle model and its equations were treated, which were used in writing the Matlab code.
The Kalman filter will be explained, first in general then a comparison will be made through different types of Kalman filters; the linear Kalman filter, the EKF (extended Kalman filter) and the UKF (perfume-free Kalman filter). All the sensors used and the approach chosen will be explained in detail. In addition, a brief introduction to the code and the steps followed will be described.
In the second part of the thesis, however, the results obtained are shown by comparing only the kinematic model to the dynamic model to which the filter is applied and comparing the latter to the true value of the sideslip angle obtained by using the optical sensor. This project takes on even more value because the optical sensor for estimating the sideslip angle is a very expensive sensor and the validation of this model allows a significant reduction in terms of costs.
In order to make the model as universal as possible, tests were carried out both for vehicles with internal combustion engines and with electric engines, making a dynamic comparison of the results obtained.

Table of Contents

List of Figures

Index of Tables

Chapter 1

1. Introduction

Vehicle Dynamics is the field of study that deals with understanding and evaluating the performance of the vehicle in terms of its response to the inputs received from the driver on a given road. We talk about ride performance when we want to analyze, from the point of view of vertical dynamics, the response of the vehicle, considered on elastic suspensions, while it moves stably on a given road surface. Instead, we speak of handling performance when, following the application of an input by the driver, the ability to drive and steer the vehicle more or less easily, while maintaining stability and control, is evaluated. Often the concept of handling is incorrectly expressed using other terms such as cornering ability and directional response which, however, express profoundly different concepts. They define objective properties of the vehicle when it changes its trajectory and exhibits lateral acceleration: the concept of cornering ability defines the level of maximum lateral acceleration that the vehicle can sustain in a stable condition, while directional response means the time of response of the vehicle, in terms of lateral acceleration, following a change in the steering angle. The understanding of the vehicle dynamics and of the investigated phenomena can take place following two different approaches: empirical and analytical. The empirical understanding of the phenomena underlying the vehicle dynamics occurs following the implementation of various experimental tests and subsequent errors through which it is possible to identify the factors that influence the performance of the vehicle under certain conditions. This approach, however, often leads to erroneous assessments, as it does not provide any information on how any changes in the vehicle's design could affect its performance. On the contrary, the analytical approach allows to describe the mechanics of the phenomena of interest using known physical laws, thus obtaining analytical models, consisting, in the simplest cases, of algebraic and differential equations that relate forces and motions of interest with input variables and vehicle or tire properties. These models therefore make it possible to identify the changes necessary to achieve certain performance objectives. However, these models, in order to be more easily manageable, present a series of approximations such that they provide a non-detailed description of reality, but only an approximate one, so that they too can lead to making errors of evaluation if they do not know each other properly. in-depth the assumptions underlying the model. To date, thanks to the greater computational capacity of computers, known the models that describe the behavior of each component of the vehicle, it is possible to assemble them in order to obtain a more complex model, which allows to simulate the behavior of the complete vehicle or any of its subsystem before this is physically realized in its components. In this way it is possible to evaluate the importance of the various parameters by including these in the model and observing the influence they have on performance after analyzing the simulated behavior of the vehicle.

1.1 The role of vehicle dynamics within the systemic design of the vehicle

The goal of a systemic approach to vehicle design is to define the technical specifications of each component, so that the vehicle, as a whole, performs its functions in the manner provided and the objectives assigned. In particular, by technical specifications we mean a series of quantities and the relative measures, designed to define, in a complete way, each component, even in the absence of detailed drawings. A systemic approach to design also makes it possible to carry out a project, however complicated, by dividing the activities that make it up between teams that operate in parallel, assigning to each of them understandable objectives, which can be independently verified and aimed at obtaining overall performance. Finally, systemic design constitutes the initial phase of each project, during which the possibility of achieving the objectives set is verified and is commonly known as a feasibility study. Within the overall design of a vehicle, the Vehicle Dynamics Development Process takes place before the prototype of the car is physically built and essentially involves three phases.

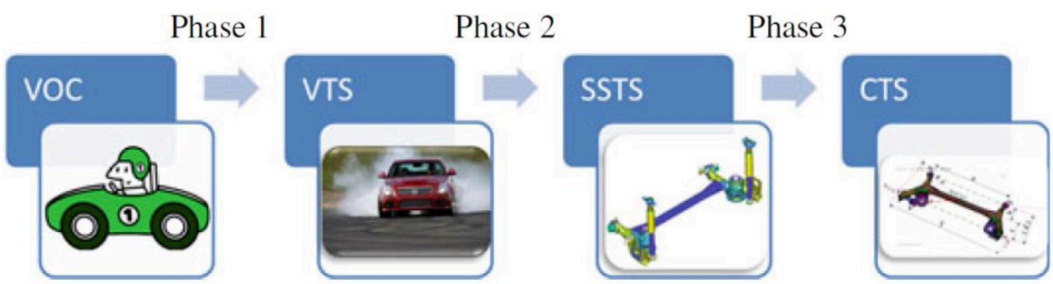

Figure 1-1 Vehicle dynamics development process.

The first phase consists in defining "qualitative" performance objectives, consistent with the type of car to be built (Subcompact car, Compact car, Sports car, Super car, Mini SUV, Compact SUV, etc.). They are defined not only on the basis of the experience gained in past projects by the team working on the project, but also by evaluating what are the demands of consumers and market trends. These qualitative targets are called VOC (Voice of Costumers) and refer qualitatively to the desired performance in ride and handling, but also in terms of speed, safety, reliability and fuel consumption. At this point, after having defined the specific technical-engineering quantities of vehicle dynamics, the compilation of particular matrices, known as Quality house, allows to identify, through the use of a particular symbology, the degree of influence that each quantity has on the previously defined VOC performance targets.

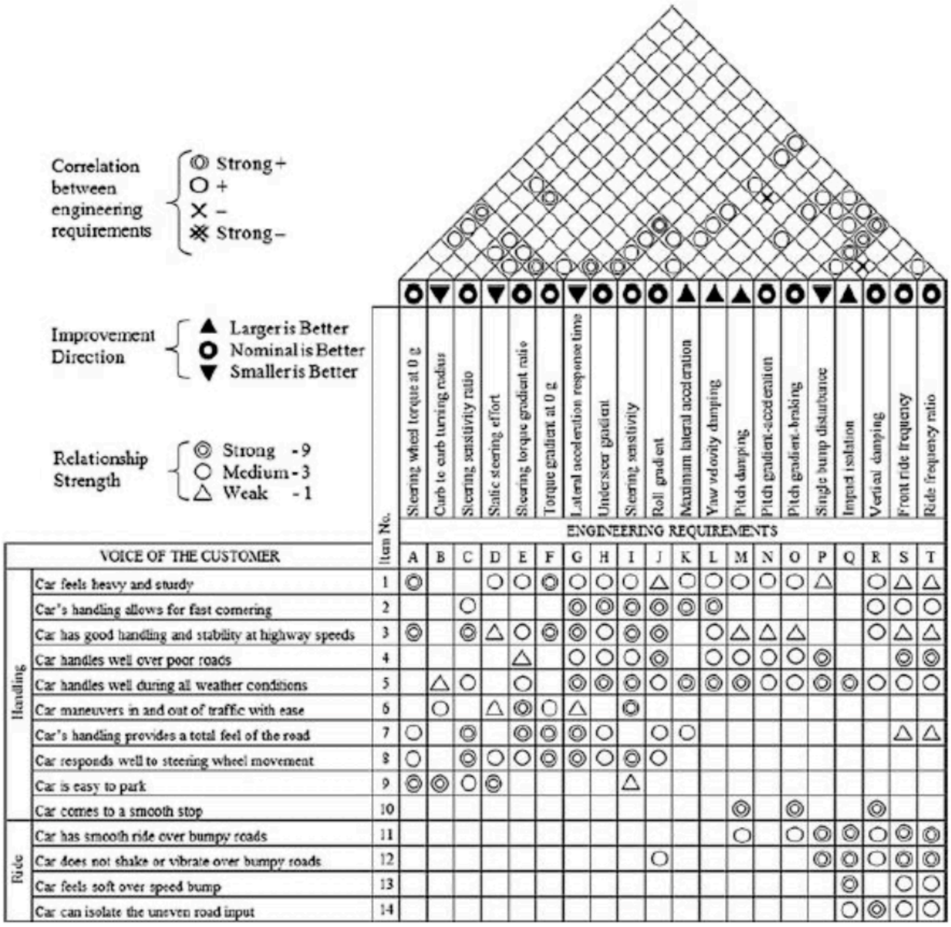

Figure 1-2 Matrix, known as the Quality House, reports the degree of correlation between VOC and VTS

These tables also make it possible to evaluate, again from a qualitative point of view, the degree of correlation existing between the various vehicle dynamics quantities. This makes it possible to translate the initial performance objectives (VOC), defined qualitatively, into technical-engineering requirements, at the vehicle level, defined, instead, from a quantitative point of view and known as VTS (Vehicle Technical Specifications). Subsequently, if we consider the vehicle as the result of the assembly of a series of subsystems (suspension systems, steering system, transmission, traction system, etc.), the second phase involves identifying, at the subsystem level, the appropriate technical requirements, known as SSTS (Subsystem Technical Specifications) which must be developed starting from the VTS defined previously. This phase requires a series of simulations, carried out both at the subsystem level and at the complete vehicle level, which allow to obtain data useful for achieving the desired performance objectives. Finally, the third phase deals with translating the SSTS into project requirements and parameters necessary for the physical realization of each component that contributes to the formation of the subsystem to which it belongs. This phase, compared to the previous one, requires much more accurate and precise modeling and simulation tools, in order to understand in depth the effects on the dynamic performance of the vehicle, complete with the design parameters of each key component of the chassis. At the end of the third phase, therefore, at the component level, the project specifications, known as CTS (Component Technical Specifications), are obtained to communicate to suppliers. Once the physical prototype of the vehicle has been created, experimental tests are carried out to verify the validity of the simulations carried out in the previous phases and the satisfaction of the performance objectives. Subsequently we proceed, both at the complete vehicle and component level, with the chassis tuning phase: the goal is to refine the design specifications of the components while trying to balance and balance the various chassis design parameters to meet the vehicle specifications. Specifications often undergo changes since, especially in this primordial phase of prototype construction, the project develops over time. The causes can be multiple: issues of durability, discrepancies between the results obtained in simulation and those deriving from experimental tests, new market trends. So, although the vehicle dynamics development process is carried out before the physical prototype of the car is built, it is good to iterate the process in order to obtain the optimal configuration of the project. The theory reported in the current chapter has been extrapolated from the sources [1], [2], [3].

1.2 Lateral dynamic of the vehicle

The study of the lateral dynamics of the vehicle is particularly linked to the safety of the driver. Active safety systems, such as ESC (Electronic stability control) are based on the study of the quantities related to this type of dynamics. One of the most important quantities involved is certainly sideslip angle. The knowledge of these quantities has also allowed, in addition to improvements in the safety field, an important advance for the handling of vehicle. In recent years, research centers and Universities are collaborating to greatly improve the vehicle's behavior to make the vehicle safer.

The development of the control systems is necessary because the human reactivity to the unexpected dangers may not be high. The control system installed on the vehicle are based on an IMU inertial measurement controller, which is linked to an accelerometer and is able to evaluate the acceleration values in the three directions of the vehicle and the rotation speeds in the same directions. The vehicle, in accordance with what is written above, is described as a body with six degrees of freedom.

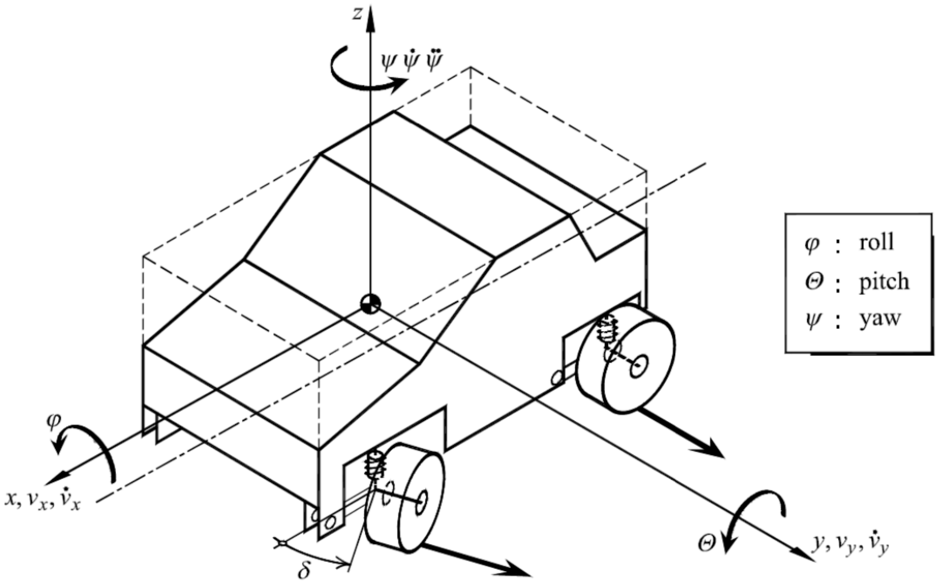

Figure 1-3 Body with six degrees of freedom

This thesis aims to estimate the sideslip angle which is defined as the angle generated between the speed vector in a generic point of the vehicle and the longitudinal direction; As a rule, the velocity vector is evaluated in the center of gravity of vehicle.

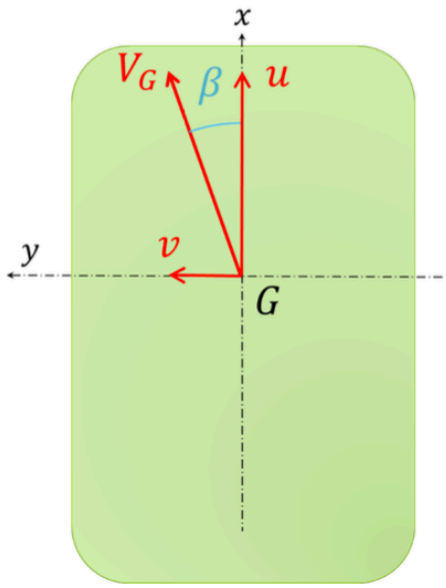

Figure 1-4 Definition of sideslip angle

In the literature several methods are available. The assumptions of each method make it more or less accurate. It is therefore impossible to find the model that is the most reliable of all. It is possible to identify two lines of research for estimation of sideslip angle [8]:

- Observer-based: This approach uses a model to estimate the state of the dynamic system. As the complexity of the model varies, it is possible to obtain the state variables more or less accurately. Based on the complexity of the model and its constituent equations, a more or less computational burden will be required. The study of these systems is complicated because, like all vehicle models, they base their reliability on a large number of parameters. In particular, as will be shown in the next chapters, wheel-to-ground contact is particularly challenging to describe as a model.

- Neural network-based: This more innovative approach is widely used in many fields of vehicle dynamics as they can estimate parameters or recognize images without any prior knowledge. Therefore, the model allows to treat the vehicle as a black box and to directly define input-output relationships. Nowadays, artificial neural networks (ANN) are widely used in any field, such as vehicle control, trajectory prediction, process control and natural resource management. Neural network-based models also offer decisive benefits such as adaptive learning, fault tolerance and generalization. This method has a hard issue to overcome, every time the system changes, the ANN must be changed, re-performing the training procedure. The observer-based seems to be preferred in car testing phase, however the ANN might be useful when the vehicle development is made.

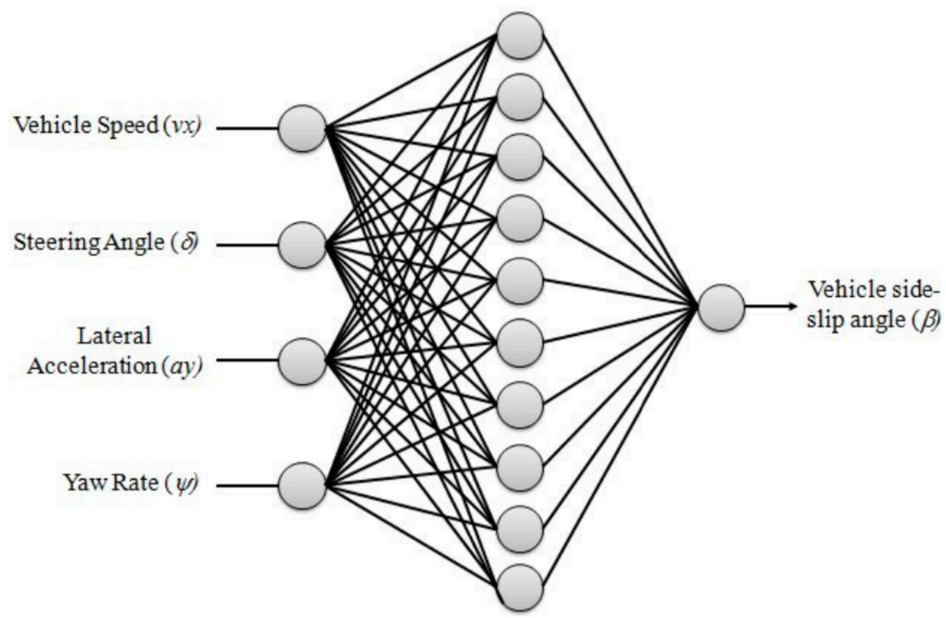

Figure 1-5 General layout of an ANN used for vehicle sideslip angle (VSA) estimation

Another methodology under development is the ANFIS [9]. The ANFIS system estimates a "pseudo heel angle" through parameters that can be easily measured using real vehicles equipped with sensors (inertial sensor and steering wheel sensor) and this value is introduced in UKF to filter the noise and minimize the variance the estimate of the mean square error. The ANFIS based observer combines the advantages of neural networks and fuzzy logic [24]. The former is adaptive and can learn from generalization and pattern recognition. The latter allows for smooth and consistent performance.

1.3 Thesis Purpose

The aim of the thesis is to build a model that, starting from input data obtainable from normal cars, estimates the sideslip angle so that, if there were any dangerous situations activate the active driving safety systems. A further objective to be achieved is that of maintaining a low computational consumption model which is at the same time reliable and economical. The tool used for the building of this model was Matlab, sometimes with the help of some internal FCA software.

1.4 Thesis Outline

Chapter 2

The second chapter of this thesis analyzes with great attention the vehicle dynamics model which is the basis for the building of the Matlab file. Secondly, is shown the discretization of the model, a process necessary for the transition from equations to analytical models. Finally, the pneumatic wheel contact model used was also defined, to highlight the complexity of the variables involved and therefore the need to build simpler models, which can reduce calculations to a minimum.

Chapter 3

In this chapter the Kalman filter and its application for vehicle dynamics have been analyzed in detail. The analysis starts from the description of the mathematical and physical model of the filter and ends with the use of it with the models described in the previous chapter. A small space has also been left for further applications, sometimes still vehicular, where the Kalman filter is becoming increasingly popular.

Chapter 4

Testing and instrumentation in the automotive sector represent the key to research. It is necessary to know the functioning and mechanisms of the basic instrumentation that allow the acquisition of tests. The same knowledge of the execution of the tests is discussed in this chapter with reference to the rules from which they were taken.

Chapter 5

This chapter explains how the algorithm works for estimating the sideslip angle. Both stationary and unsteady tests were analyzed to make the algorithm universal and capable of evaluating vehicle behavior under different driving conditions.

Chapter 6

Conclusions are discussed in this chapter. These summarize the contributions presented in the previous chapters, highlighting the future objectives of the research regarding the subject matter.

Chapter 2

2. Vehicle Model Theory

The first step in using a Kalman filter that estimates the sideslip angle is the definition of a dynamic model for the vehicle. Over the years, the development of dynamic models has been increasingly important for estimating the characteristic parameters of the car and for car simulations.

The formulation of a model is particularly complicated and depends on the simplifications used. In fact, the same vehicle could be studied as a series of sub-models that describe in a more or less appropriate way particular vehicle behaviors subject to situations.

The physical quantities that will be used in the algorithms for estimating the sideslip angle are the following:

- δ_v: Steer angle;
- u_n: Longitudinal velocity;
- a_y: Lateral acceleration;
- a_x: Longitudinal acceleration;
- $\dot{\psi}$: Yaw rate;
- $\dot{\vartheta}$: Roll rate;
- $\dot{\phi}$: Pitch rate.

In addition to these parameters, it is necessary to introduce the slip angle α which is connected to the sideslip angle. The slip angle is defined as the angle generated between the longitudinal direction of the vehicle and the speed vector in the wheel center.

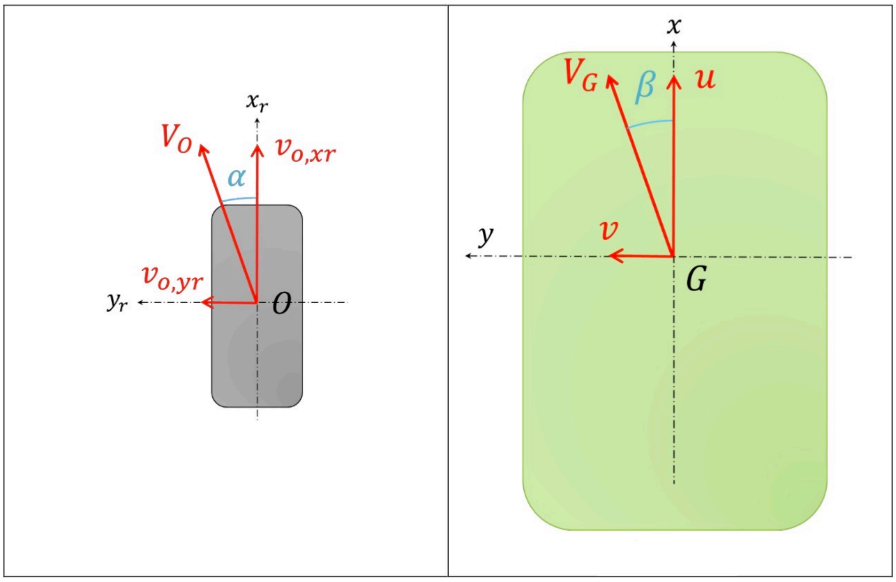

Figure 2-1 To the left the slip angle, to the right the sideslip angle

As widely described in the previous chapter, the purpose of this thesis is to generate a model that can estimate the sideslip angle starting from the quantities that are known in a common car. The common sensors that are present in the car are the following:

- **GPS** for calculating the speed of the car
- **Gyroscope** capable of evaluating the angle speed in the 3 directions
- **Accelerometer**: a sensor that is implemented at the **IMU** that measures the accelerations in the 3 directions. It is usually positioned near the gearbox.
- Measurement sensor for the steering angle.

Chapter 4 illustrates the operation and structure of these sensors in detail.

2.1 Kinematic Model

Considering the vehicle as a rigid body moving in an x-y plane, it is possible to derive the following relationship which describes the link between the two acceleration components of the vehicle's center of gravity (longitudinal a_x and lateral a_y) and the speed components with respect to reference jointed to the vehicle [10].

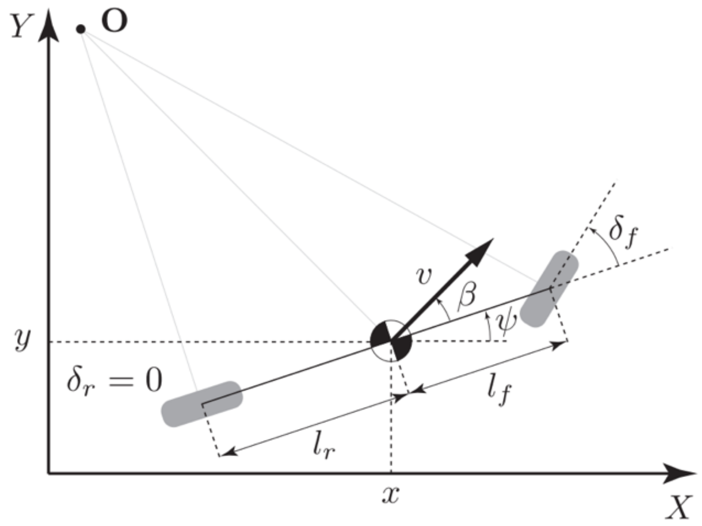

Figure 2-2 Kinematic Model Scheme

The velocity vector $\vec{V}$, defined in the center of gravity of the vehicle itself, can be decomposed into two components which are:

$$\vec{V} = \vec{u} + \vec{v} = u\,\hat{\tau} + v\,\hat{n} \tag{2.1}$$

- $\vec{u}$ is the tangential component of the velocity vector;
- $\vec{v}$ is the normal component of the velocity vector.

By definition the acceleration $\vec{a} = \frac{d(\vec{v})}{dt}$, it follows that:

$$\vec{a} = \left(\dot{u} - \dot{\psi}v\right)\hat{\tau} + \left(\dot{v} + \dot{\psi}u\right)\hat{n} \tag{2.2}$$

From the following equation we obtain

$$\begin{cases} a_x = (\dot{u} - \dot{\psi}\,v) \\ a_y = (\dot{v} + \dot{\psi}\,u) \end{cases} \tag{2.3}$$

By integrating, we obtain the relationship that connects speed and acceleration

$$\begin{cases} u = \int\left(a_x + \dot{\psi}\,v\right)dt \\ v = \int\left(a_y - \dot{\psi}\,u\right)dt \end{cases} \tag{2.4}$$

In matrix form

$$\binom{\dot{u}}{\dot{v}} = \begin{bmatrix} 0 & \dot{\psi} \\ -\dot{\psi} & 0 \end{bmatrix}\binom{u}{v} + \binom{a_x}{a_y} \tag{2.5}$$

From this model known the value of u and v, it is possible to calculate the value of the sideslip angle which by definition is equal to:

$$\beta = arctang\left(\frac{v}{u}\right) \tag{2.6}$$

Clearly the use of such a simplified model involves the presence of errors, which are already incorporated in the hypotheses of the model itself.

2.2 Single Track Model

Lateral dynamics contemplates the study of the dynamic behavior of a vehicle during cornering and more generally during changes of direction. In the case of cars, the driver acts on the steering wheel which changes the slip angle of the steering wheels (normally the front wheels), producing lateral forces. These forces modify the sideslip angle of the entire vehicle (variation of β) thus also setting the rear wheels in drift and thus generating the necessary driving forces [4].

To schematize lateral dynamics, the simplest model is the bicycle model (also known as single track model). The hypotheses on which the bicycle model is based are:

- The vehicle moves on a horizontal plane, so there is no slope of any kind;
- The wheels of each axle are condensed into a single equivalent wheel;
- The vehicle speed is set constant, providing for a decoupling between longitudinal and lateral dynamics;
- The steering, slip angle and sideslip angles are small $\alpha_f, \alpha_r, \delta, \beta \rightarrow 0$;
- The curve radius of the trajectory is greater than the wheelbase of the car: R >> L;
- Linear behavior of lateral forces $F_y = C_\alpha \alpha$;
- Load transfer effects are neglected.

The vehicle parameters to be known, in addition to those already presented for the kinematic model, are:

- The mass of the vehicle M;
- The inertia evaluated in the center of gravity J_z;
- The position of the center of gravity and the definition of the wheelbase of vehicle;
- The slip stiffnesses of the axles $C_{\alpha_{front}}, C_{\alpha_{rear}}$.

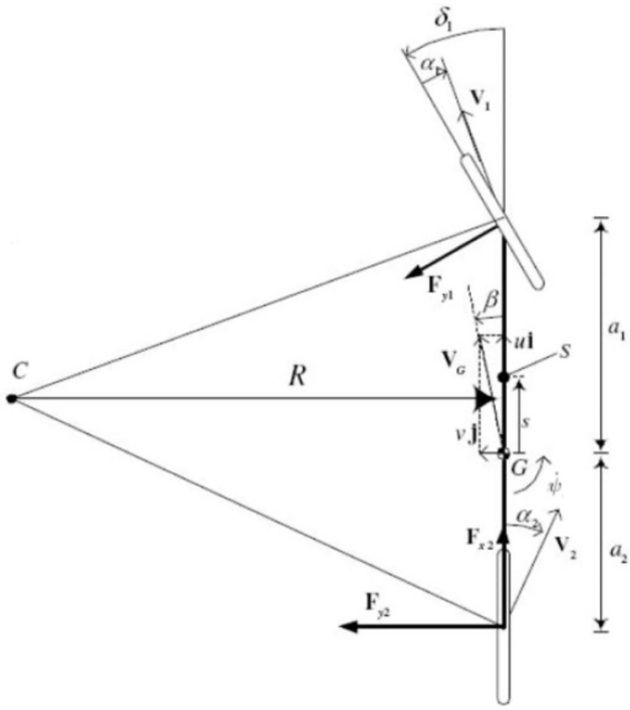

Figure 2-3 Single track model

It is also assumed that the steering axal is only the front ones, therefore $\delta_2 = 0$. Making the balance of force and moment of the scheme *Figure 2-3*.

$$\begin{cases} \mathrm{m\ a_y = F_{y_2} + F_{y_1}\cos(\delta_1)} \\ \mathrm{J_z\ddot\psi = a_1 F_y \cos(\delta_1) - a_2 F_{y_2}} \end{cases} \tag{2.7}$$

These equations can be simplified thanks to the hypothesis of small angles of the bicycle model therefore $\cos(\delta) \approx 1$ and $F_y = C_\alpha\ \alpha$

Furthermore, it has been seen that $\alpha = \delta - \beta$

The expression 2.7 thanks to the hypotheses becomes:

$$\begin{cases} m(\dot v + \dot\psi\ u) = C_{\alpha_1}\left(\delta_1 - \frac{v+\dot\psi a_1}{u}\right) + C_{\alpha_2}\left(-\frac{v-\dot\psi a_2}{u}\right) \\ J\ddot\psi = C_{\alpha_1} a_1\left(\delta_1 - \frac{v+\dot\psi a_1}{u}\right) - C_{\alpha_2} a_2\left(-\frac{v-\dot\psi a_2}{u}\right) \end{cases} \tag{2.8}$$

Recalling the relationship that links the steering angle with the steering wheel angle

$$\delta_1 = \delta_v \tau$$

The equation can be rewritten as follows:

$$\begin{cases} \dot v = Y_v v + Y_{\dot\psi}\dot\psi + Y_\delta \delta_v \\ \ddot\psi = N_v v + N_{\dot\psi}\dot\psi + N_\delta \delta_v \end{cases} \tag{2.9}$$

Whose parameters are:

$$Y_v = -\left(\frac{C\alpha_1 + C\alpha_2}{mu}\right) \tag{2.10}$$

$$Y_{\dot{\psi}} = -\left(\frac{C_{\alpha_1}\alpha_1 + C_{\alpha_2}\alpha_2}{mu} + u\right) \tag{2.11}$$

$$Y_\delta = \left(\frac{C_{\alpha_1}\tau}{m}\right) \tag{2.12}$$

$$N_v = -\left(\frac{C_{\alpha_1}\alpha_1 - C_{\alpha_2}\alpha_2}{J_z u}\right) \tag{2.13}$$

$$N_{\dot{\psi}} = -\left(\frac{C_{\alpha_1}\alpha_1^2 + C_{\alpha_2}\alpha_2^2}{J_z u} + u\right) \tag{2.14}$$

$$N_\delta = \left(\frac{C_{\alpha_1}\alpha_1\tau}{J_z}\right) \tag{2.15}$$

In general, a dynamic system can be expressed as a formulation of the state space as follows:

$$\dot{x} = [A]\{x\} + [B]\{u\}$$

- x is the vector of the states, that is the vector that contains the parameters that dynamically define the system
- *u* is the vector of the inputs, which in this case represents the value of the flying angle

If the parameters of u and v were constant over time, the matrices [A] and [B] would be constant. In this case the result would be an LTI system (linear dynamic system with invariable time).

The equation (2.8) is not linear with respect to the parameters u, v. It is necessary to linearize the following parameters:

$$\frac{v}{u};\ \frac{\dot{\psi}}{u};\ \dot{\psi}u$$

Linearization is the extension of the linearization of a curve with respect to a straight line, but in two dimensions.

$$f(x)f(y) = f(x_o)f(y_0) + f'(x_o)(x - x_o)f(y_o) + f'(y_o)(y - y_o)f(x) \tag{2.16}$$

Solving the calculations:

$$\begin{cases} \dot{v} = Y_v v + Y_{\dot{\psi}}\dot{\psi} + Y_u u + Y_\delta \delta_v + K_2 \\ \ddot{\psi} = N_v v + N_{\dot{\psi}}\dot{\psi} + N_u u + N_\delta \delta_v + K_3 \end{cases} \tag{2.17}$$

$$Y_v = -\left(\frac{C_{\alpha_1}+C_{\alpha_2}}{mu_o}\right) \tag{2.18}$$

$$Y_{\dot{\psi}} = -\left(\frac{C_{\alpha_1}a_1+C_{\alpha_2}a_2}{mu_o}+u_o\right) \tag{2.19}$$

$$Y_u = \frac{C_{\alpha_1}v_o+C_{\alpha_1}\dot{\psi}_o a_1-C_{\alpha_2}\dot{\psi}_o a_2+C_{\alpha_2}v_o}{mu_o^2}-\dot{\psi}_o \tag{2.20}$$

$$Y_\delta = \left(\frac{C_{\alpha_1}\tau}{m}\right) \tag{2.21}$$

$$K_2 = -\frac{C_{\alpha_1}v_o+C_{\alpha_1}a_1\dot{\psi}_o+C_{\alpha_2}v_o-C_{\alpha_2}a_2\dot{\psi}_o}{mu_o^2}+\dot{\psi}_o u_o \tag{2.22}$$

$$N_v = -\left(\frac{C_{\alpha_1}a_1-C_{\alpha_2}a_2}{J_z u_o}\right) \tag{2.23}$$

$$N_{\dot{\psi}} = -\left(\frac{C_{\alpha_1}a_1^2+C_{\alpha_2}a_2^2}{J_z u_o}\right) \tag{2.24}$$

$$N_u = \frac{C_{\alpha_1}v_o a_1+C_{\alpha_1}\dot{\psi}_o a_1^2-C_{\alpha_2}\dot{\psi}_o a_2^2+C_{\alpha_2}v_o a_2}{J_z u_o^2} \tag{2.25}$$

$$K_3 = -\frac{C_{\alpha_1}v_o a_1+C_{\alpha_1}a_1^2\dot{\psi}_o+C_{\alpha_2}v_o a_2-C_{\alpha_2}a_2^2\dot{\psi}_o}{J_z u_o} \tag{2.26}$$

$$N_\delta = \left(\frac{C_{\alpha_1}a_1\tau}{J_z}\right) \tag{2.27}$$

The structure obtained is the same as that seen previously but with the presence of a K term that takes account of the parameters where the linearization was performed.

$$\dot{x} = [A]\{x\}+[B]\{u\}+[K]$$

Thanks to this procedure the matrices A.B, K are constant as they are independent of u and v; however, the points of linearization $u_o, v_o, \dot{\psi}_o$ appear.

As regards the lateral speed and the yaw speed, since they assume very small values around zero, it is plausible that their linearization around a constant value does not lead to large changes in the results; this is not practicable for u_o. The longitudinal speed during the test could vary a lot, which makes it difficult to choose the correct parameter u_o which gives adequate results. Because of this it is necessary to introduce alternative models, based, as will be seen, on the Kalman filter that eliminate the following problem.

2.3 Discretization of model

To solve the problem, it is necessary to update the linearization point step by step, and therefore it is necessary to switch from continuous systems to a discrete system.

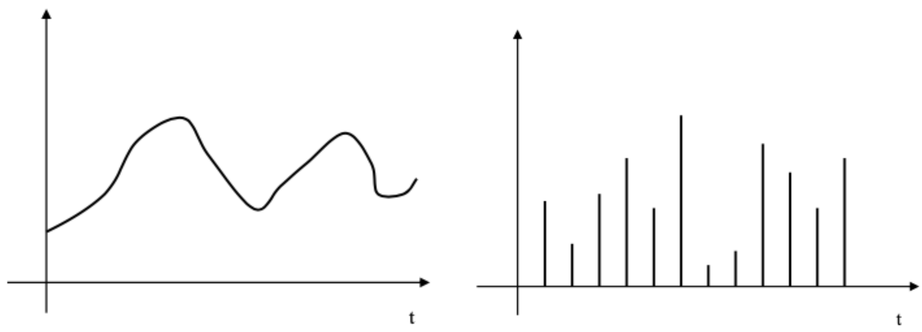

Figure 2-4 To the left continuous signals, to the right discrete signal

It is possible to switch from continuous systems to discrete systems by dividing the time domain into small intervals, thus defining the x_k samples that represent the state of the system at that given instant.

The equations making up the model are differential equations; a first order derivative is then introduced using the forward Euler formula:

$$\dot{x} = \frac{dx}{dt} = \frac{x_{k+1} - x_k}{T_s}$$

- T_s is the sampling time
- x_k is the state of the system at k-th instant.

2.3.1 Kinematic Model Discretization

The relations used for the discretization of time can be applied to the two models mentioned above;

$$\begin{cases} \dot{u} = \dot{\psi} v + a_x \\ \dot{v} = -\dot{\psi} u + a_y \end{cases} \tag{2.28}$$

Applying Euler

$$\begin{cases} \frac{v_{k+1} - v_k}{Ts} = -\dot{\psi}_k u_k + a_{y_k} \\ \frac{u_{k+1} - u_k}{Ts} = \dot{\psi}_k v_k + a_{x_k} \end{cases} \tag{2.29}$$

By organizing members:

$$\begin{cases} v_{k+1} = v_k - Ts\dot{\psi}_k u_k + Ts\, a_{y_k} \\ u_{k+1} = u_k + Ts\, \dot{\psi}_k v_k + Ts\, a_{x_k} \end{cases} \tag{2.30}$$

In matrix form:

$$\begin{pmatrix} u_{k+1} \\ v_{k+1} \end{pmatrix} = \begin{bmatrix} 1 & Ts\,\dot{\psi} \\ -Ts\dot{\psi} & 1 \end{bmatrix} \begin{pmatrix} u_k \\ v_k \end{pmatrix} + \begin{bmatrix} Ts & 0 \\ 0 & Ts \end{bmatrix} \begin{pmatrix} a_{x_k} \\ a_{y_k} \end{pmatrix} \tag{2.31}$$

By defining x as the state vector of the system and u as the generic vector of inputs

$$x_{k+1} = A_k x_k + T_s B u_k$$

The matrix A, called the stiffness matrix, is variable for each k-th step, while B remains constant.

2.3.1 Dynamic Model Discretization

Recalling the equation of single track model (2.17) applying Euler and writing everything in matrix form:

$$\begin{pmatrix} v_{k+1} \\ \dot{\psi}_{k+1} \end{pmatrix} = \begin{bmatrix} 1 + T_s Y_v & T_s Y_{\dot{\psi}} \\ T_s N_v & 1 + T_s N_{\dot{\psi}} \end{bmatrix} \begin{pmatrix} v_k \\ \dot{\psi}_k \end{pmatrix} + \begin{bmatrix} T_s Y_u & T_s Y_\delta \\ T_s N_u & T_s N_\delta \end{bmatrix} \begin{pmatrix} u_k \\ \delta_{v_k} \end{pmatrix} + \begin{pmatrix} T_s K_2 \\ T_s K_3 \end{pmatrix} \tag{2.32}$$

In generic form:

$$x_{k+1} = A_{dyn} x_k + T_s B_{dyn} u_k + T_s K$$

In this case, A, being linearized, is a constant that does not depend on the k-th instant. If we wanted to use the non-linearized model equations we would obtain the following structure:

$$\begin{pmatrix} v_{k+1} \\ \dot{\psi}_{k+1} \end{pmatrix} = \begin{bmatrix} 1 + T_s Y_v & T_s Y_{\dot{\psi}} \\ T_s N_v & 1 + T_s N_{\dot{\psi}} \end{bmatrix} \begin{pmatrix} v_k \\ \dot{\psi}_k \end{pmatrix} + \begin{pmatrix} Y_\delta \\ N_\delta \end{pmatrix} \delta_v \tag{2.33}$$

And so the state space form is:

$$x_{k+1} = A_k x_k + T_s B u_k$$

2.4 Tyre Model

This paragraph explains the mechanics of the tire by introducing the basic concepts for the generation of the contact force between tire and ground, proposing two possible models; in the literature it is possible to find many other models that have the aim of describing in an even more accurate way what happens to ground wheel contact [4] [7].

The difference between a tire and a rigid wheel is the deformability of it. From a dynamic point of view, however, the law that can be written in both cases is the following:

$$C = F_x R + I\ddot{w} \tag{2.34}$$

The tire has the ability to deform under stress. Therefore, to the normal radius R of the tire, a loaded radius R_l is added, that is the radius of the tire if a forcing F_z is applied on it.

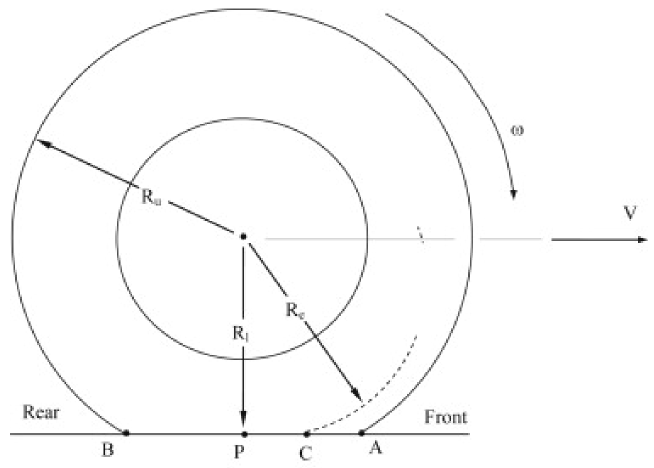

Figure 2-5 Tyre model

The contact forces F_x and F_y between the tyre and the ground depend on a multitude of parameters.

The most common are proposed:

- Pressing force F_z;
- Coefficient of adhesion μ;
- Temperature T;
- Tyre wear;
- Tyre pressure.

2.4.1 Brush Model

The brush model considers the tire as constituted by many bristles, one parallel to the other, having a particular elastic characteristic defined by a stiffness parameter that links the tension to the deformation.

$$\tau = k\rho \tag{2.35}$$

The term ρ in this case indicates the deformation. If we refer to a lateral deformation the equation becomes:

$$\tau_y = k_y\, w \tag{2.36}$$

If we refer to a longitudinal deformation the equation becomes:

$$\tau_x = k_x\, u \tag{2.37}$$

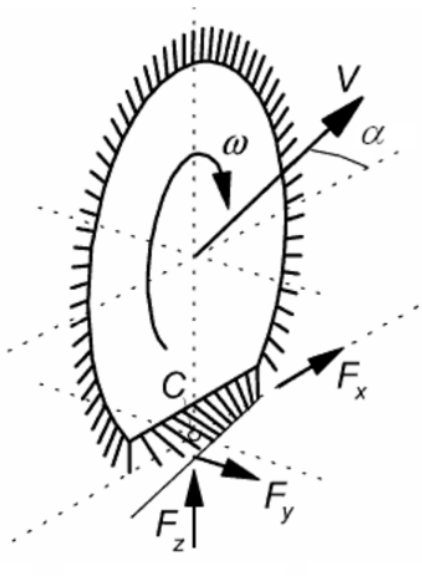

Figure 2-6 Brush Model Scheme

The considerations have been made for the case of lateral deformation, however in a similar way it would happen for the longitudinal deformation. The assumptions on which the brush model is based are the following [8]:

- Independence between the various bristles;
- Parabolic contact pressure distribution;
- Non-deformability of the case;
- Rectangle contact area according to precise proportions.

Assuming a case of zero sliding σ, the displacement of the bristles at a slip angle α is equal to:

$$w(\xi) = -\alpha\,\xi \qquad (2.38)$$

Recalling that $T_y = \int \tau_y \, dA = \int -\tau_y \, \alpha \, \xi \; dA$ up to the conditions of adhesion;

and that $T_y = -f_d \; p(\xi)$ after the adhesion limit; the tangential force is obtained.

The figure shows the trend of the lateral force as the slip angle varies.

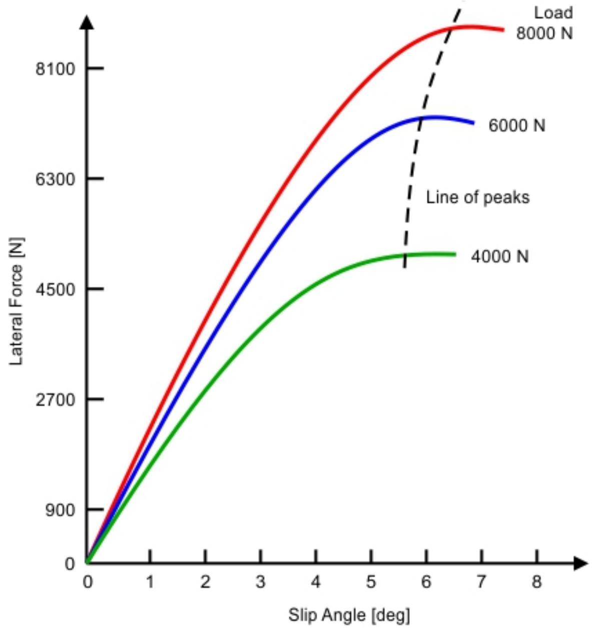

Figure 2-7 Trend of lateral force as the slip angle varies for 3 types of tyre

The *Figure 2-7* shows a linear proportionality in the first section between lateral force and slip angle. The brush model is an excellent model which, through simple relationships, allows you to obtain good feedback with reality. However, the hypotheses on which it is based are particularly stringent, therefore empirical models that have greater precision are often preferred.

2.4.2 Pacejka's Model

The modeling of a tyre can generally be carried out based on two distinct procedures: one by creating a physical-theoretical model, aimed at physically justifying and quantifying the phenomena that affect the dynamics of the tire; the other involves the creation of an empirical-mathematical model with the aim of reproducing the characteristic behaviors of the real component, based on mathematical formulas created ad hoc following experimental characterizations, independent of the physical reality that determines the behavior acquired through the measurements.

An empirical-mathematical model is generally less complex and easier to integrate into models that describe the dynamics of the vehicle; while a physical-theoretical model, starting from a physical study and being therefore based on laws and equations that try to represent reality, is more complex but also potentially suitable for conducting a detailed analysis of the performance of a tire in relation to construction parameters.

An example of a physical-theoretical model is the brush model previously analyzed, capable of physically justifying the phenomena that generate the tire-soil force exchanges; while the empirical-mathematical model that we want to present is one of the most important, perhaps the most widespread in the automotive field, known as "Pacejka Magic Formula", introduced in 1987 by HB Pacejka.

The "Pacejka Magic Formula" is therefore an empirical-mathematical model that tries to summarize the experimental performance of the tire through mathematical formulas. These have a precise structure in which quantified coefficients appear on the basis of specific experimental tests.

By inserting these coefficients into the formula, obtained for a specific tire, it is possible to obtain the characteristic curves of the tire itself, with a more or less high level of approximation as the operating conditions vary. In general, these curves allow to obtain the trends of the actions determined with the brush model:

- Longitudinal force F_x;
- Lateral force F_y;
- Moment of self-alignment M_z

as a function of the longitudinal sliding s (also known as σ), the slip angle α and the camber angle γ.

By observing the experimental curves of the characteristics of a tire, it can be seen that they remain similar to each other as the operating conditions of the tire itself vary. This is equivalent to saying that the curves obtained by making the input and output quantities dimensionless (for example, α and F_y respectively) and by varying the operating conditions, are almost identical.

This particular characteristic of the tire dynamics guarantees a high level of approximation of Pacejka's Magic Formula compared to the experimental data, within certain ranges of operating conditions.

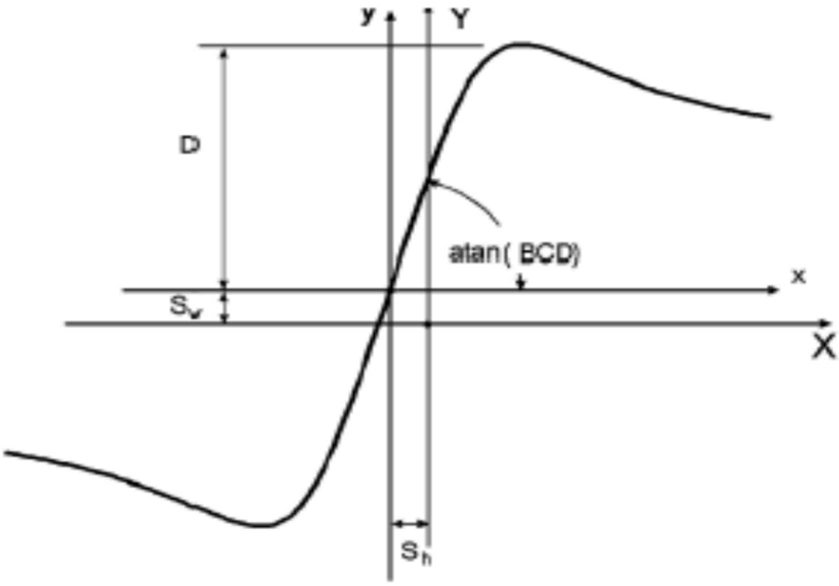

Figure 2-8 Pacejka's Magic Formula

$$Y = D\, sin\left[C\, arctang\left(Bx - E\big(Bx - arctang(Bx)\big)\right)\right] \qquad (2.39)$$

- B Stiffness Factor;
- C Shape Factor;
- D Peak Factor;
- E Curvature Factor

The curve represented *Figure 2-8* in has offsets with respect to the origin (S_H and S_V), due to phenomena not covered in this thesis, but which affect the dynamics of the tire; among these are the residual self-alignment moment M_{zr}, the conicity and the ply-steer. For example, the latter two cause the wheel to transmit lateral forces to the ground even in the absence of a slip angle, as shown in *Figure 2-9*.

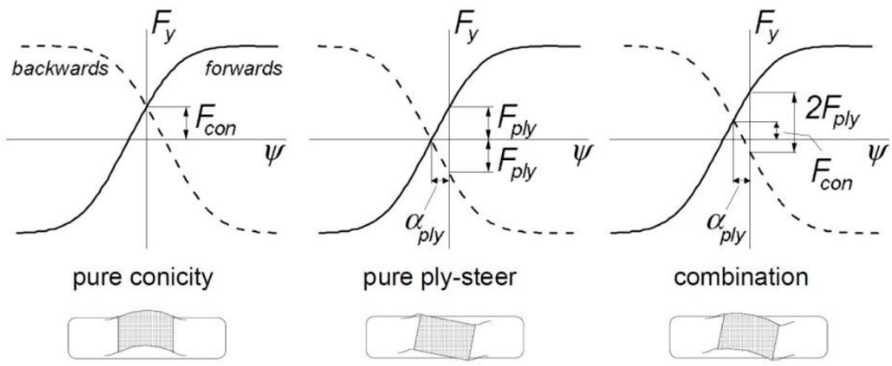

Figure 2-9 Influence of conicity and ply-steer phenomena on F_y

2.4.3 Models for transient behavior

Previous models are able to describe the behavior of the tire at steady state and therefore at constant speed. In fact, the calculated forces correspond to the values that the tyre develops after the transient settling. However, it was necessary to introduce a model that would also validate what happened in the transient. The key concept for the transient model is the relaxation length L. This parameter is the distance that the pneumatic wheel must travel to guarantee the generation of the force (63%) foreseen by the kinematic condition. On average, stationary conditions are reached after a distance of 3L [4].

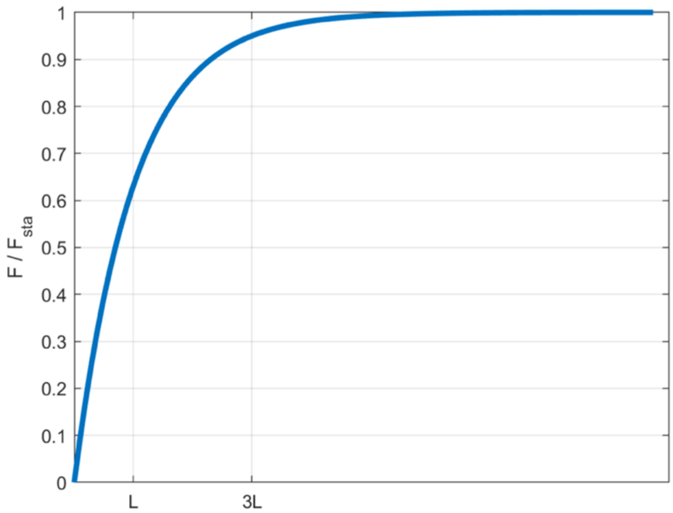

Figure 2-10 Force step response

The trend of the force shown in the *Figure 2-10* represents the response to a step assuming it as a first order force according to the following law:

$$\frac{L}{V}\dot{F} + F = \bar{F} \tag{2.40}$$

$$\tau = \frac{L}{V} \tag{2.41}$$

$$\frac{F_{rit}}{F_{pac}} = \frac{1}{\tau S + 1} \tag{2.42}$$

If the vehicle speed was constant, the equation solved and reported in the time domain would be the following:

$$F(t) = F_o\left(1 - e^{-\frac{t}{\tau}}\right) \tag{2.43}$$

Chapter 3

3. Kalman Filter

As fully explained in the previous chapters, the estimate of the sideslip angle of a car and the consequent formation of the model is something far from simple and immediate. In fact, some parameters that are difficult to calculate are present in the matrices. It was necessary for the creation of a model which is as precise as possible the introduction of Kalman filter, that is a mathematical tool that evaluates the state of the system starting from a series of measurements subject to noise and a dynamic model of the system.

The filter is normally used when the variable of interest is not directly measurable and must be estimated starting from measurements of other parameters.

3.1 History of Kalman Filter

The filter is named after its inventor Rudolph Emil Kalman, who in 1960 published an article describing a recursive solution to the linear filtering problem of discrete data. Since that time, due in part to significant advances in digital computing, the Kalman filter has been the subject of research and applications, particularly in the area of autonomous or assisted navigation. One of its first applications was in the Apollo project to estimate the trajectory of spacecraft to the moon and back.

3.2 Description of Kalman Filter

The Kalman filter requires:

- A series of measures of the system to be estimated;
- Knowledge of a linear mathematical model of the system.

The effect of the filter on the analyzed quantities is given by two contributions, one predictive and one corrective

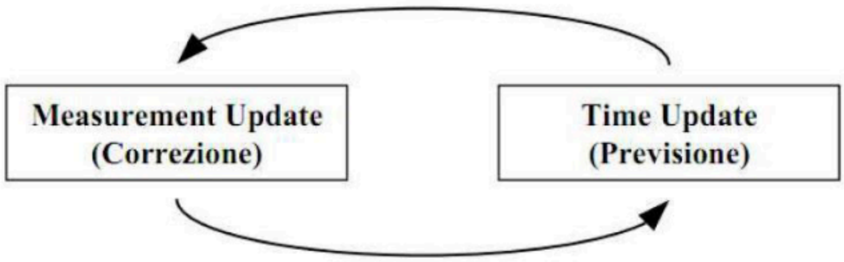

Figure 3-1 Logic diagram of the filter

The equations of the system model provide a forecast, while those of the "measurement update" correct the forecast; The logic cycle as indicated in the *Figure 3-1* is very simple; the information contained by the measurement is entered, the result will be sent to the predictive model which, based on the input data, will provide the forecast for the next instant.

The Kalman filter needs a linear dynamic model, which can be described according to the state formulation as:

$$\dot{x} = Ax + Bu$$

A second equation must be added to this equation which relates the vector of states x to the vectors of the available states (i.e. those obtainable from the measurement).

$$y = Cx$$

- x: state vector of dimension n
- y: vector of available states of dimension m (with $m \leq n$)
- u: vector of the inputs to the system of dimension l

The matrices A, B and C therefore link the predictive model to the measurement model.

The Kalman filter can be applied both on continuous linear dynamic models and on discrete dynamic models;

Therefore, once a sampling time T_s has been set, the equations seen above become:

$$\begin{cases} x_k^p = A_k x_{k-1} + T_s B_k u_{k-1} \\ y_k = C\, x_k^p \end{cases} \tag{3.1}$$

The subscript p indicates that the vector was obtained from the predictive block and will be subsequently corrected.

The corrective block takes as input the prediction of the state vector x_k^p and corrects it through the measure vector y_k. In simple terms it compares the model prediction and the true measure to get the best estimate of the model parameters. A problem with this model is the need to attribute weights to the relative contributions (measurement and prediction) in order to give greater importance to one or the other block. What is written can be translated into analytical relationships by introducing covariance matrices.

Q, the **covariance matrix of the model**, is defined as the matrix that quantifies the variance of the error linked to the model.

$$Q = \begin{bmatrix} w_{k_1} & 0 & \dots & 0 \\ 0 & w_{k_2} & 0 & \dots \\ \dots & 0 & \ddots & 0 \\ 0 & 0 & 0 & w_{k_n} \end{bmatrix} \quad [nxn] \tag{3.2}$$

The lower the w_{k_i} are, the more reliable the model is.

Instead, **R** is defined as the **covariance matrix of the measurement**, or the matrix that quantifies the variance of the error linked to the measure.

$$R = \begin{bmatrix} z_{k_1} & 0 & \dots & 0 \\ 0 & z_{k_2} & 0 & \dots \\ \dots & 0 & \ddots & 0 \\ 0 & 0 & 0 & z_{k_n} \end{bmatrix} \quad [mxm] \tag{3.3}$$

The lower the z_{k_i} values, the more reliable the measurements are. Usually we proceed with the identification of the relationship between the two matrices $\frac{w_{k_i}}{z_{k_i}}$; the smaller this parameter is, the more value is given to the model.

Starting from these two matrices we define the Kalman covariate matrix which varies step by step such that:

$$P_k^i = A_k P_{k-1}^f A_k^T + Q \tag{3.4}$$

- A is the model matrix.

Once the covariance matrix is obtained, it is possible to obtain the main parameter for the Kalman correction filter, that is the **Kalman gain**.

$$K_k = P_k^i C^T \left(C P_k^i C^T + R\right)^{-1} \tag{3.5}$$

The Kalman gain is used to correct the prediction of the state vector

$$x_k = x_k^p + K_k\left(y_k - C x_k^p\right)$$

x_k represents the definitive estimate of the states of the System and it contains both the theoretical and the measurement model. Finally, it will be possible to update the value of the covariance matrix at the end of the path through the following relationship:

$$P_k^f = [I - K_k C] P_k^i [I - K_k C]^T + K_k R K_k^T \tag{3.6}$$

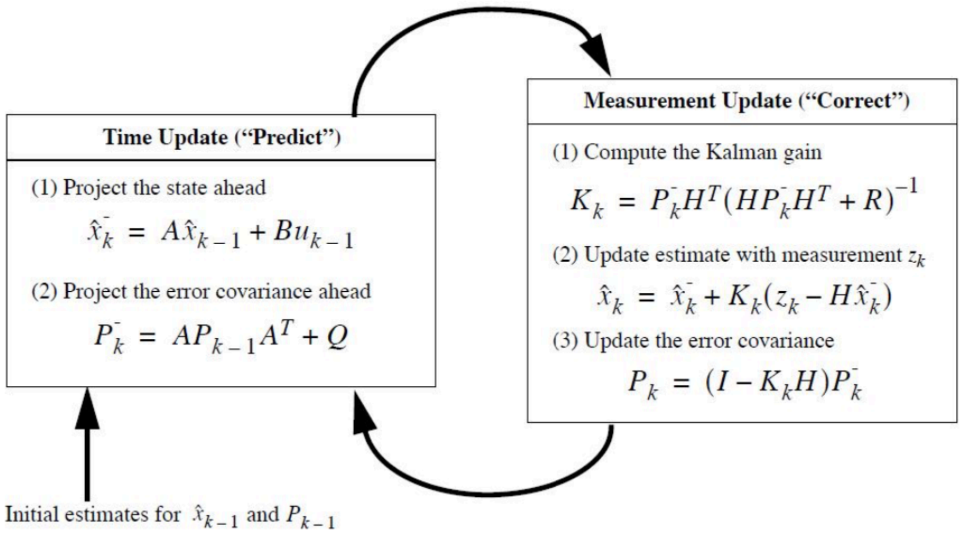

Figure 3-2 Summary of Kalman's operations

The Kalman filter (KF) requires a mathematical linear model of the system.

Nonlinear problems can be solved with the extended Kalman filter (EKF). This filter is based upon the principle of linearization of the state transition matrix and the observation matrix with Taylor series expansions. Exploiting the assumption that all transformations are quasi-linear, the EKF simply makes linear all nonlinear transformations and substitutes Jacobian matrices for the linear transformations in the KF equations. The linearization can lead to poor performance and divergence of the filter for highly non-linear problems.

An improvement to the extended Kalman filter is the unscented Kalman filter (UKF). The UKF approximates the probability density resulting from the nonlinear transformation of a random variable. It is done by evaluating the nonlinear function with a minimal set of carefully chosen sample points. The posterior mean and covariance estimated from the sample points are accurate to the second order for any nonlinearity [8].

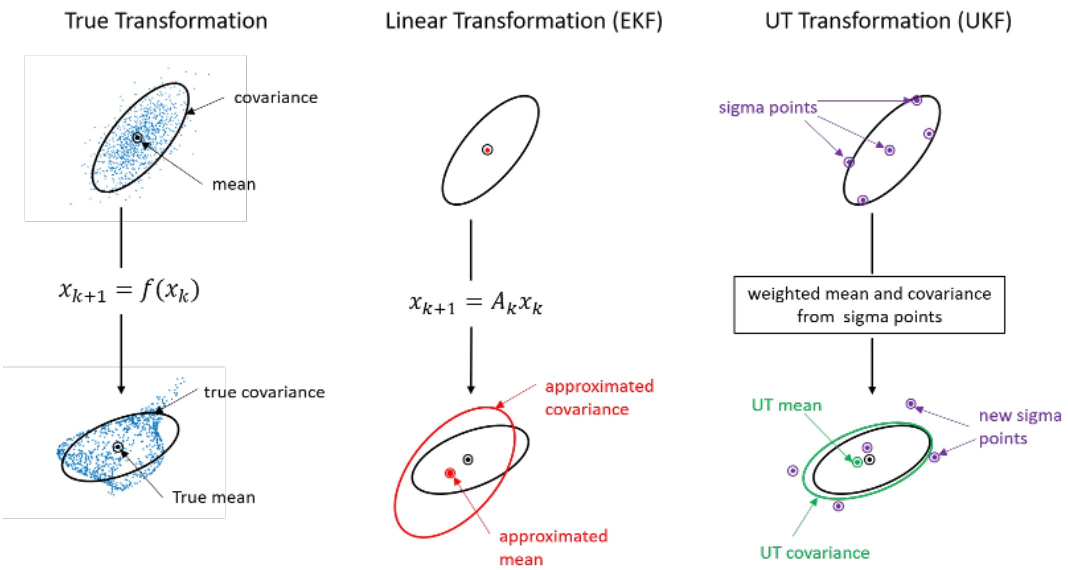

Figure 3-3 Different Types of Kalman Filter

From the above presentation, it is clear that the Kalman UKF filter is the best solution for any problem (linear and non-linear). However, one goal of this thesis is to build a model that has a low computational load. Therefore, the use of the KF is preferred rather than the UKF.

Type of filter	KF	EKF	UKF
Complexity	Medium	High	Very high
Computational burden	Low	Medium	High
Working range	Medium	High	Very high

Table 3-1 Characteristics of different Kalman Filters

3.3 Filter application to the vehicle model

The Kalman filter is a recursive filter [7] applicable for any system that is described by a linear model; The following paragraph will explain the application of the filter to the vehicle model.

3.3.1 Kinematic Filter

The application of the Kalman filter to the kinematic model takes the name of Kinematic filter. Recalling the equation (2.31)

$$\begin{pmatrix} u_{k+1} \\ v_{k+1} \end{pmatrix} = \begin{bmatrix} 1 & Ts\,\dot{\psi} \\ -Ts\dot{\psi} & 1 \end{bmatrix} \begin{pmatrix} u_k \\ v_k \end{pmatrix} + \begin{bmatrix} Ts & 0 \\ 0 & Ts \end{bmatrix} \begin{pmatrix} a_{x_k} \\ a_{y_k} \end{pmatrix}$$

defining x as the state vector of the system is the generic vector of the inputs:

$$x_{k+1} = A_k x_k + T_s B u_k$$

the system inputs u are:

- lateral acceleration a_y;
- longitudinal acceleration a_x.

These quantities are in fact measured directly by the accelerometer.

The x states of the system are:

- Longitudinal speed u;
- Lateral speed v.

The only state available y of the system is the longitudinal speed u, as it is the only state of the system for which there is a direct measurement to compare. (in reality the available state is the absolute speed V but the two speeds can be confused).

$$y = u = [1 \quad 0]\, x$$

The measurement of system is:

- lateral acceleration a_y;
- longitudinal acceleration a_x;
- Longitudinal speed u;
- Yaw rate $\dot{\psi}$.

3.3.2 Dynamic Filter

The application of the Kalman filter to the dynamic model (single track model) takes the name of Dynamic filter. The discretization of the model is (2.32)

$$\begin{pmatrix} v_{k+1} \\ \dot{\psi}_{k+1} \end{pmatrix} = \begin{bmatrix} 1 + T_s V_2 & T_s R_2 \\ T_s V_3 & 1 + T_s R_3 \end{bmatrix} \begin{pmatrix} v_k \\ \dot{\psi}_k \end{pmatrix} + \begin{bmatrix} T_s U_2 & T_s D_2 \\ T_s U_3 & T_s D_3 \end{bmatrix} \begin{pmatrix} u_k \\ \delta_{v_k} \end{pmatrix} + \begin{pmatrix} T_s K_2 \\ T_s K_3 \end{pmatrix}$$

In generic form

$$\mathrm{x_{k+1} = A_{dyn} x_k + T_s B_{dyn} u_k + T_s K}$$

For the matrix linearization performed, the term K goes to zero if they are chosen as linearization internals for the rotational speed and lateral velocity. In this case the inputs u of the system are:

- Longitudinal speed u;

- Steer angle δ_v.

Which are measured directly by the GPS and the steering wheel angle sensor system. The states of system x instead are:

- Lateral speed v;
- Yaw rate $\dot{\psi}$.

The available state y of the system is the yaw rate

$$y = \dot{\psi} = [0 \quad 1]x$$

It was possible to create a Simulink model that would show in a synthetic way what was seen in an analytical way

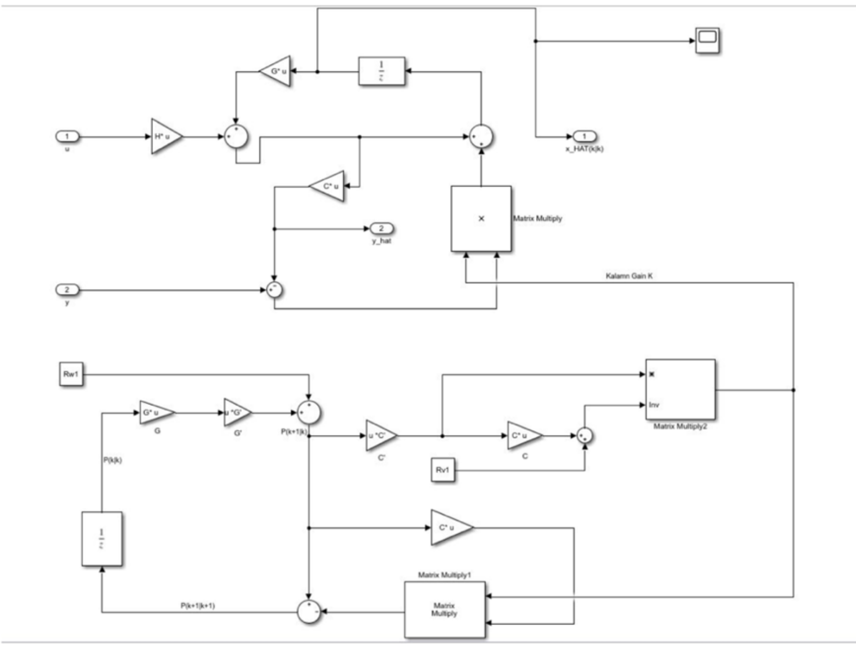

Figure 3-4 Kalman filter in Simulink

3.4 Other application of Kalman Filter

From the description it is possible to notice the immense applications that the Kalman filter can have in the automotive sector, which includes not only the dynamic aspects but also the motorsport ones; In the literature there are innumerable researches that show the applications in this field and in the evolution of the Kalman filter in a more complex filter that takes the name of corpuscular theory; F. Asghar, M.Talha uses the Kalman filter to estimate the SOC (state of charge) of battery in automotive field [11]. P.Block uses filter Kalman and Particle filter for robot navigation [12]; and also in the robotic field, the Kalman filter is having strong developments [13].

Chapter 4

4. Testing and instrumentation procedure

Testing vehicles is complex. Therefore, it was necessary to insert some tests and regulated procedures that would allow in a repeatable and objective way to understand the dynamic characteristics of the vehicles. The purpose of these dynamic tests is therefore to test the vehicles to achieve the objectives in terms of VOC, VTS set.

4.1 Balocco Experimental Center

The Balocco Experimental Center (*Figure 4-1*) is a complex of car circuits located near Balocco (VC), built by Alfa Romeo and currently owned by Stellantis Group.

Figure 4-1 Circuits of Balocco Experimental Center

Construction work began in 1961 by Alfa Romeo, and the first circuits were inaugurated in 1962; the original project included a main track (the current Mixed Alfa Romeo), within which to create a smaller track, as well as areas with special paving and the reproduction of a country road.

When the Stellantis Group bought Alfa Romeo, the circuit came into the possession of the Turin-based company. Under the new management, the plant has undergone major changes, which have given it several new tracks, with different characteristics and purposes. Today there are the following tracks:

- The high-speed ring, a 7.8 km long trioval, with elevated curves characterized by a gradient of up to 30%, which allows maximum speeds of over 300 km/h;
- The Langhe route, a reproduction of a secondary road (inspired by the Langhe region), with numerous escape routes and variants that allow for different routes. It measures over 22 km, and is characterized by the unevenness of the road surface and the numerous ups and downs (slopes up to 14%), designed to undermine the set-up of the cars to be tested;
- Comfort track, with flooring designed for suspension testing;
- ABS track, used for the homologation of vehicles;
- Off road track;
- White track, created for the purpose of simulating low grip conditions to test the active safety systems installed on vehicles;
- Steering Pad; circular square of 80 m in diameter with a slope of 2% towards the interior, made with three different types of asphalt;
- Noise track, used for vehicle approval;
- IVECO ring, dedicated to high-speed testing of IVECO heavy vehicles.

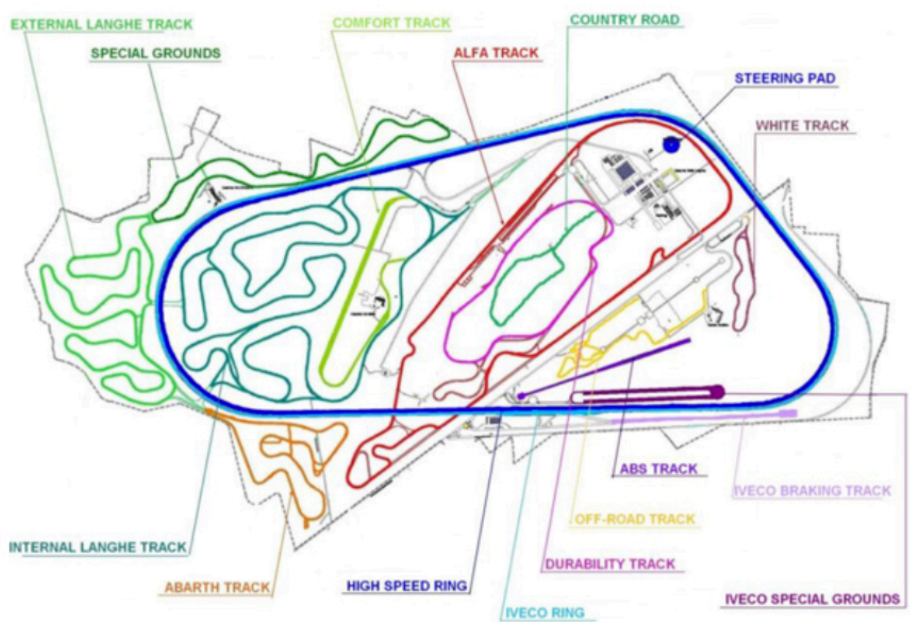

Figure 4-2 Layout of circuits of Balocco Experimental Center

4.2 Maneuvers description

The term Handling refers to the drivability and maneuverability of a vehicle. The performance of a vehicle in this sense is typically analyzed by means of regulated maneuvers, divisible by different criteria.

A first subdivision is based on the state of the car that wants to be analyzed during the test. Therefore:

1. **steady state**: in which the car is analyzed in the moments of equilibrium, in particular when the steering wheel angle and speed are constant. The steady state maneuvers are all performed by traveling along a curvilinear trajectory with a constant radius at a constant speed;

2. **transitory state**: the analysis is focused on the moments when the car is not in equilibrium, that is when the longitudinal and/or lateral speed of the vehicle is varied by means of accelerator and steering inputs.

Another classification is instead made based on the input given to the vehicle by the driver who intervenes on the steering wheel, gearbox, accelerator and brake:

1. The maneuver is said in **open loop** when the input is preset, regardless of the result it generates;

2. When, on the other hand, the driver manipulates the vehicle controls in order to make the vehicle travel a certain trajectory or to reach certain values for the physical quantities involved (such as, for example, lateral acceleration), a **closed loop** operation.

The application of ISO standards and robust legacy test procedures are good practices for the implementation of a reliable testing process. The "minimal" set of tests, which are defined by ISO standards, are covering the main aspects of vehicles behavior on lateral, longitudinal and cross-coupled dynamics, as shown in the Fig.4.3.

Here a list of the main standard maneuver:

- Slow increasing steers: constant speed, steering wheel angle increases till the car limits;
- Steering pad: constant turn radius, speed increases till the car limits;
- SIN: constant speed and frequency, sinusoidal steering wheel angle input;
- RSI: constant speed, frequency sweep steering wheel angle input;
- SAC: constant speed while steering wheel angle increases, sinusoidal input;

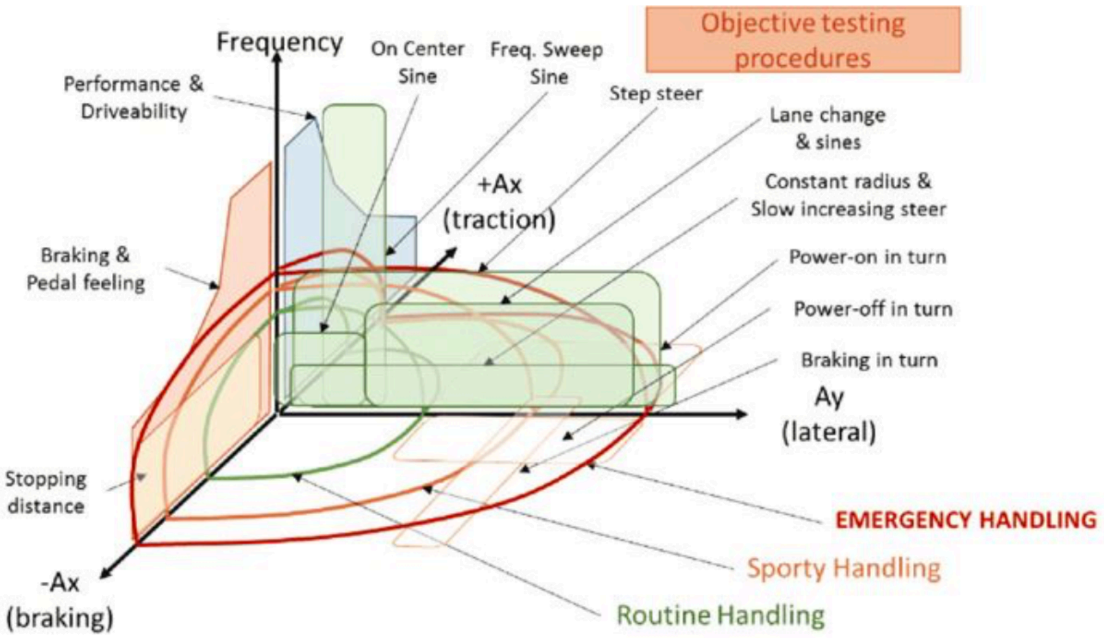

Figure 4-3 ISO standard maneuvers

- Step Steer: constant speed, step input, steering wheel stays constant until the stationary condition is reached;
- CPS: step steer input is maintained for a few seconds;
- DLC: double lane change input (double CPS).

A brief description of the main maneuvers by ISO normative are introduced, in the next pages.

4.2.1 Sinusoidal steering wheel cycles (ISO 7401)

The standard values for nominal speed are 60 km/h and 120 km/h.

Test execution:

At constant nominal speed (default 60km/h and 120km/h) and nominal gear (IV gear) it collects a steering wheel sinus with frequency 0.2Hz and a nominal

amplitude, corresponding to a peak lateral acceleration (a_y) of 0.2g and 0.4g.

The sinus is made of three parts:

- Initial offset part;
- The sinus wave;

- Final offset

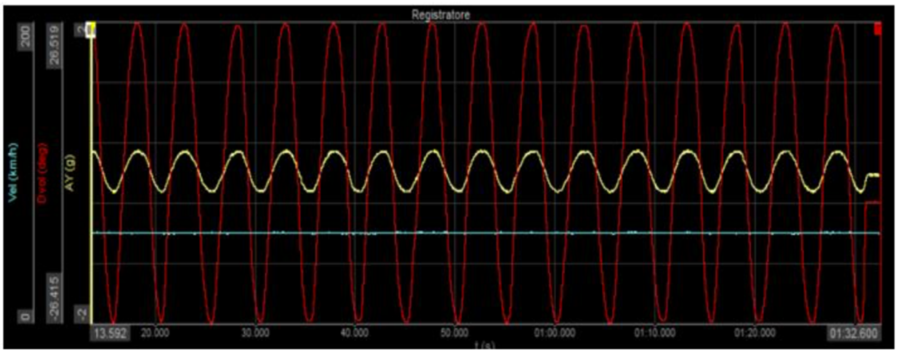

Figure 4-4 Sinusoidal steering wheel cycles with u = 60km/h ay = 0.25g

Threshold for acceptability:

- Difference between nominal speed (usually 60km/h and 120km/h) and test medium speed (VEL) < 2.0km/h
- Steering angle sinus frequency 0.2 Hz ± 0.1 Hz;
- 0,2g < Peak lateral acceleration <0,25g.

4.2.2 Sweep steering wheel input (ISO7401)

This test shall be performed at least at three different amplitudes of steering wheel angle. The amplitude of the steering wheel angle may be a reference value for steering wheel angle or a value corresponding to a desired steady state lateral acceleration.

The standard value for nominal speed is 120 km/h, depending on the different market segments and so on for the lateral acceleration amplitude levels according to car classification, following this scheme:

- Speed = 120km/h - Lateral Acceleration = 0.3g – 0.5g – 0.7g

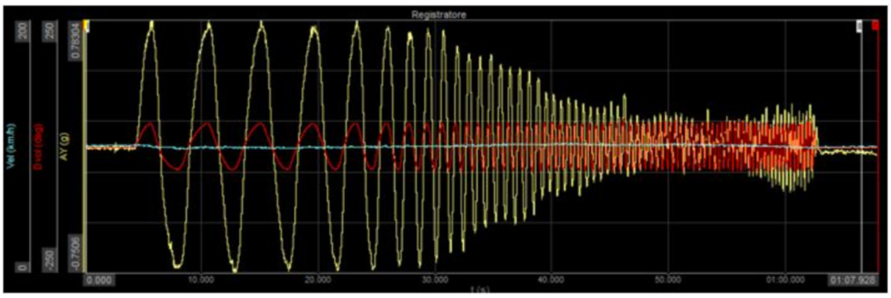

Figure 4-5 Sweep steering wheel input with u = 120 km/h ay = 0.7g

Test execution:

At constant nominal speed it collects a steering wheel sinus with increasing frequency from 0.2 Hz to 4 Hz and constant amplitude corresponding to the desired steady state lateral acceleration. The wave is made of three parts:

- Initial offset
- Increasing frequency sinus wave
- Final offset

4.2.3 Step steering input tests (ISO 7401) and steering wheel release

The standard value for nominal speed is 100km/h. According to the vehicle requirements and road friction coefficient, different speeds may be used, preferably in 20 km/h steps, as well as different steering wheel angles.

Test execution:

The maneuver is made of four parts:

- Initial offset on straight line at constant nominal speed;
- Step steer, then steering wheel angle constant;
- Steering wheel release;
- Final offset on straight at constant speed or with vehicle stopped.

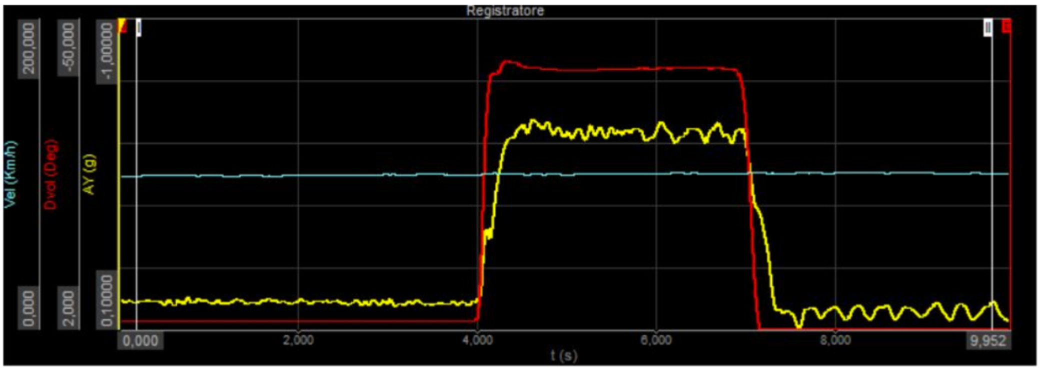

Figure 4-6 Step steering and steering wheel release u=100km/h

The test shall be performed in IV gear, at constant gas pedal position, if not differently specified. It might be made at different steering wheel angle. It must be payed attention to avoid overshoot of steering wheel angle after the step and keep steering wheel as constant as possible for at least 3 seconds, then release the steering wheel and let the vehicle self-align.

4.2.4 Slow increasing steer

This comprehends also quasi-steady state behavior in the linear range. The standard value for initial speed is 100 km/h and the steering wheel angle shall increase with a rate of 30°/s up to 180°.

Test execution:

The maneuver is made of four parts:

- Initial offset on straight at constant nominal speed
- Steering wheel angle ramp, increasing at a rate of 30°/s, up to 180° (duration = 6s)
- Hold final constant value (duration > 3 s)
- Final offset on straight or vehicle stopped (duration >2 s)

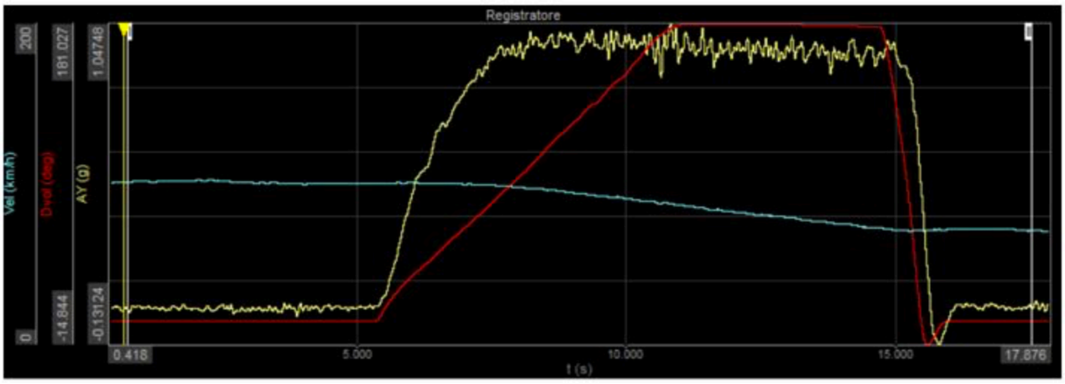

Figure 4-7 Slow increasing steer u=100km/h

During the initial offset, the steering-wheel shall be subject to zero steer torque input. The recommended method to achieve this is to drive the vehicle under free steering control (hands free). In the whole test the gas pedal position shall remain fixed and the test is executed in IV gear if not different specified.

Threshold for acceptability:

- Difference between nominal speed (usually 100km/h) and test initial speed (VEL) < 2.0km/h
- Steering angle speed (DVP) = 30°/s

4.3 Instruments

The instrumentation plays a key role in the acquisition of the data that will then be provided in the Matlab model. It is therefore important to know the structure and operation of the instrumentation to better understand the meaning of the testing procedure.

4.3.1 IMU

An inertial measurement unit or inertial platform (also known simply as an IMU) is an electronic system based on multi-axis combinations of precision gyroscopes, accelerometers and magnetometers, which allow for monitoring the dynamics of a moving vehicle, which can be used by the computer or on-board control unit to implement any corrective measures.

Figure 4-8 Inertial platform

All components are combined in one case and only a 4-wire cable leads to the connector. All sensor data is transferred to the data logger via a bus line. The inertial measurement unit measures up to six dimensions: yaw, roll and pitch, as well as lateral, longitudinal and vertical accelerations. The measuring element of the yaw rate sensor works according to the Coriolis principle, which means that it uses the inertia force of an oscillating mass in a rotating system. Due to the high resonant frequency of 25 kHz and the closed control and drive unit, the measuring element is very insensitive to mechanical disturbances. Acceleration is measured based on the change in capacitance in micromechanical structures.

The inertial measurement unit contributes to the functionality of the active and passive safety systems and the airbag control unit as well as to the vehicle test. The inertial measurement unit is available for a multitude of automotive applications, as well as for future advanced functions of driver assistance systems and automated driving.

4.3.2 Accelerometer

An accelerometer is a measuring instrument that can detect and / or measure acceleration. With the multiplication of applications, the types of these instruments have also increased, each with different functional and constructive characteristics. In most part of accelerometers, the principle is the same: it is based on detecting the inertia of a mass when subjected to acceleration. The mass is usually suspended thanks to an elastic apparatus, while a sensor detects its displacement with respect to the fixed structure of the device, this structure represents the inertial system for the accelerometer but not for the navigation and/or movement control system.

In the presence of an acceleration, the mass (which has its own inertia) moves from its rest position in proportion to the detected acceleration. The sensor transforms this movement into an acquirable electrical signal.

Below is a classification of accelerometers according to the principle of operation:

- Strain gauge accelerometers;
- Piezo resistive accelerometers;
- LVDT accelerometers (based on the principle of mutual induction);
- Capacitive accelerometers;
- Piezoelectric accelerometers;
- Laser accelerometers;
- Gravitometers;
- MEMS accelerometers.

In the automotive field, as regards use in an inertial platform, MEMS (Micro-Electro-Mechanical System) technology is mainly used.

4.3.3 Gyroscope

The gyroscope is a device used to detect the angular velocity of a body in an inertial space. There are several physical principles that can be the basis of the functioning of these measuring instruments and that give a first classification:

- Mechanical gyroscopes;
- Laser gyroscopes;
- Optical gyroscopes;
- MEMS gyroscopes.

4.3.4 GPS

The GNSS system (Global Navigation Satellite System) or better known as NAVSTAR GPS (Navigation Satellite Timing And Ranging Global Positioning System), represents the cornerstone of satellite positioning. Since 1984, alongside the PPS (Precise Positioning Service) for military applications only, this system has also been made available to civilian users for the first time.

The satellites make two complete orbits in a sidereal day (they are therefore non-geostationary) and are able to provide, 24 hours a day, the planimetric and altimetric position of any point on the surface of the planet, both immobile and in motion. The orbital parameters of each satellite, determined at the computer center, are combined in a message forwarded to the satellite concerned through one of the rescue stations. The satellite records the received parameters in its memory and re-radiates them to the users.

The operating principle of the GPS receiver is based on a spherical positioning method, which consists in measuring the time taken by a radio signal to travel the satellite-receiver distance. Knowing the time taken for the signal to reach the receiver and the exact position of at least three satellites to have a two-dimensional position, and four to have a three-dimensional position, it is possible to determine the position in space of the receiver itself. This procedure, called trilateration, uses only distance information and is similar to triangulation, from which it differs however in the fact that it does without information regarding the angles.

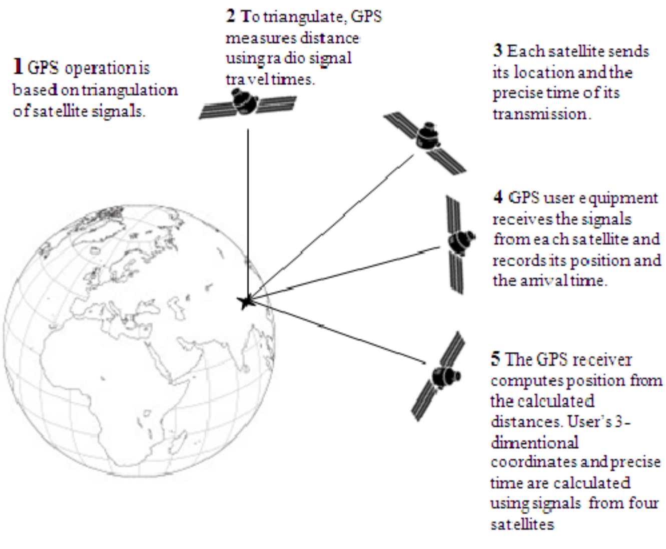

Figure 4-9 Trilateration system

4.3.4 Optical sensor

Using a high-intensity light source to illuminate the measurement surface, the optical component of the Kistler sensor observes the stochastic microstructure of the surface via an objective lens [14].

The only way to obtain a good and reliable measure of sideslip angle is to use a 2-axis optical sensor (such as Kistler) on the car, usually on the front or on the back. The instrument shines a light on the asphalt and determinates the two-speed components (u and v) obtaining so the sideslip angle.

As explained before, this instrument cannot be used on the series production vehicles and it is usually forbidden also for racing cars. For these reasons, it is necessary to find a reliable method to estimate the sideslip angle.

Figure 4-10 Example of an optical sensor (Kistler) used for vehicle dynamics testing

The acquired optical signal is projected onto a periodic prismatic grating within the system, where it is multiplied as details of the surface microstructure move across the grating.

Resultant spatial frequencies are integrated over the sensor field to generate a correlated average value. The electronic signal-processing component of the system utilizes tracking filters to determine the representative center frequency, which is derived by calculating a mean value based on the variance in the frequency spectrum. This representative center frequency allows reliable counting of signal periods, which are directly proportional to the distance that the observed surface has travelled relative to the sensor. Using this information, speed data can be derived for a gated length measurement.

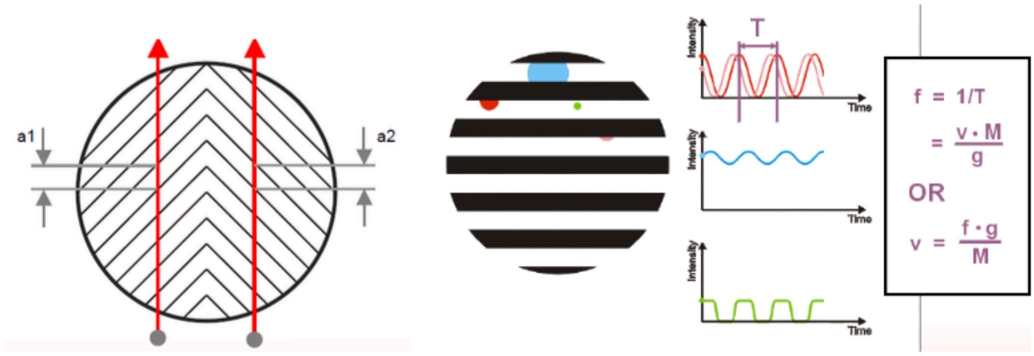

Figure 4-11 Optical sensor working principle to value u *and* v *to calculate* β

4.3.5 Universal measurement steering wheels

Steering wheels sensors are designed for automotive testing. This generation of transducers incorporates numerous technological functions, such as:

- Angle reset, torque calibration
- A Start trigger signal to the remote data acquisition system.
- Optical coder processing to prevent the need for external TTL electronics
- Five simultaneous analogue output signals
- Suppression of the bearing friction influence on torque, allowing high accuracy for low torque measurements
- Low profile design retains the same driving conditions as with standard steering wheels:
- Optional steering stops adjustable between ± 15° to ± 165° are available. These stops fold automatically for safety.

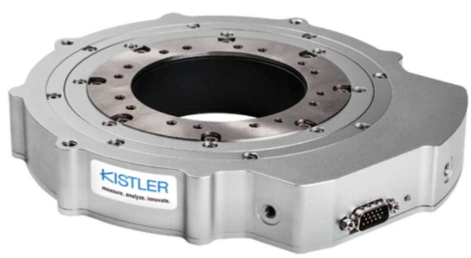

Figure 4-12 Example of an universal measurement steering wheel used for vehicle dynamics testing

4.4 Data Acquisition and Signal Processing

As anticipated, the measures are made both from CAN Network and from External sensors. In this work, either external signals and CAN Network are used for sideslip angle estimation, privileging the external sensors; this is because the precision is typically higher, furthermore it allows to be coherent with the VSA acquisition, which is possible just with the optical sensor. However, a check of the difference between the two measurement methods was done and the results is positive: the error is acceptable so that it's possible to say that the choice of one or the other signal is indifferent.

Figure 4.11 shows what said before; in the first graph is plotted the difference between the two a_y signals; it does not exceed 0.01 g and, if the CAN measure was filtered, the error would be even smaller. For the direct acquisition, the software used was: Dewesoft X. This is used especially as first interface instrument to check measurements and maneuvers, however it is sometimes used to filtering signals as well as to apply other mathematical tools.

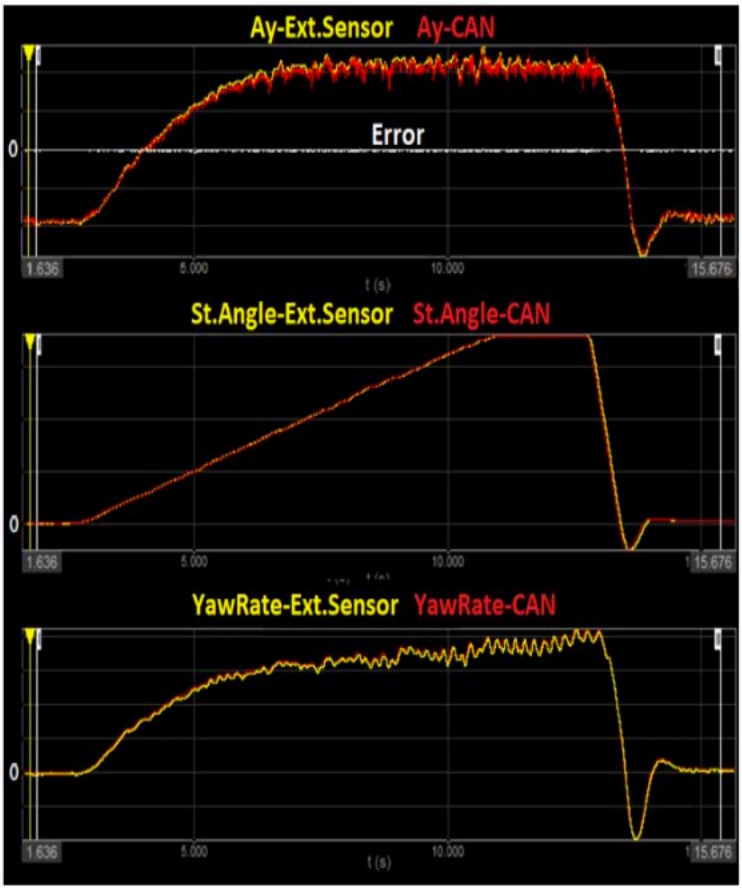

Figure 4-13 Comparison between ay, Steering angle and Yaw Rate measured by CAN and by external sensors

4.5 Introduction to hybrids

In recent years, the technology of HEVs, or electrified hybrids, has been enjoying increasing success given the increasingly stringent standards for CO_2 emissions and pollutants in general.

In this paragraph, a general introduction to HEVs is made with particular attention to the P-HEVs which will later be used to compare these to cars with ICE heat engines. This comparison will be used to optimize the Matlab file created so far. In this case we want to validate the model for a 4WD car where the rear axle is driven by the electric motor. The greater mass linked to the battery compartment causes greater lateral forces on the rear axle. The model instead was designed on an ICE AWD car. Through these tests, our aim is to make the built model even more general.

4.5.1 Description of the structure of a hybrid car

Hybrid cars combine two or more power sources that can directly or indirectly allow the propulsion of the vehicle itself. The primary source of energy is typically the chemical energy stored in the tank. When we talk about HEVs, we are defining hybrids that have electric as their second source of power.

A second major distinction that is made for the hybrid is between plug-in hybrids (P-HEVs for electric hybrids) and non-plug-in hybrids. In the first case, the battery can be recharged from the outside with a charging column while in the second case it is the heat engine that guarantees the battery sufficient charge levels. in the bibliography there are documents showing control technologies for the different types of hybrid. It should also be noted that even these motor control strategies often use the Kalman filter [18] [19].

A second distinction between hybrids must be made based on the placement of electric machines within the vehicle's transmission configuration. So, we distinguish:

- Series hybrids
- Parallel hybrids

Without going into detail, the figures of the standard configurations of series and parallel hybridization are shown.

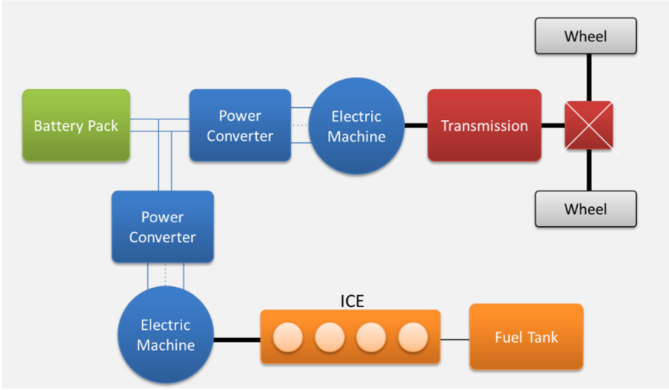

Figure 4-14 Structure series HEVs

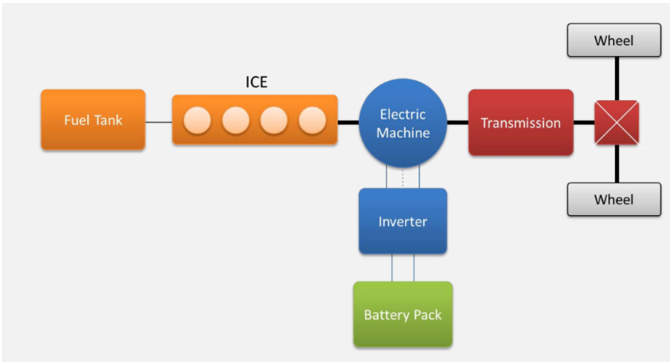

Figure 4-15 Figure 7 1 Structure parallel HEVs

For parallel hybrids, the position of the connection between the electrical part and the thermal part of the car is very important. Based on the position of the link we will distinguish the following configurations:

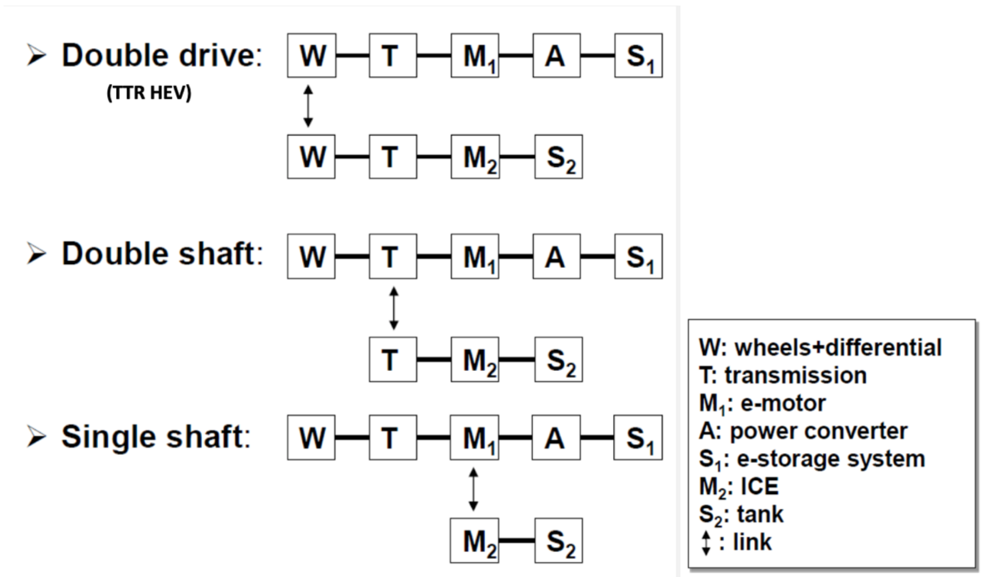

Figure 4-16 Parallel HEVs configurations based on link position

For purely economic and sometimes performance technologies, the technologies most in use at the moment are those of the single shaft and double drive. Furthermore, the research is currently proposing alternative hybrid configurations which take the name of complex hybrids [21].

4.6 Error

Once the model was tested in different situations, two parameters were computed to obtain mathematical values that might be indicative for the model accuracy. Here below explained:

- The Mean Absolute Error (MAE)
- The Root Mean Squared Error (RMSE)

The MAE is the average of the absolute difference between the measured value and the estimated one.

The RMSE represents the square root of the second sample moment of the differences between predicted values and observed ones or the quadratic mean of these differences.

$$MAE = \frac{1}{n}\sum_{i=1}^{n} | y_{measured} - y_{estimated} |$$

$$RMSE = \sqrt{\frac{1}{n}\sum_{i=1}^{n} (y_{measured} - y_{estimated})^2}$$

Therefore, at the end of each test, the improvements obtained through the built model will be validated according to the above parameters.

Chapter 5

5. Sideslip angle estimation

The goal of this thesis is to estimate the sideslip angle of the vehicle. In this chapter we refer to all the equations of the dynamic model of the vehicle seen in the previous chapters. Once the acquired data have been filtered, they are ready to be used to estimate the sideslip angle.

Below is the data sheet of the car used during the tests:

Figure 5-1 Jeep Compass

DATA SHEET	
VEHICLE	JEEP COMPASS
Traction	FWD
Steering ratio	15.6
Width [mm]	1840
Wheelbase [mm]	2636
Distance from center of mass and front axle [mm]	1057
Distance from center of mass and rear axle [mm]	1573
Mass [kg]	1700

Table 5-1 Data sheet Vehicle

5.1 Introduction to model parameters

The bicycle model was picked because it is a good compromise between its complexity and its adaptability in this specific field. Moreover, the idea behind this model is that it is not necessary or desirable to include the longitudinal vehicle dynamic, because it does not affect deeply the lateral stability of the vehicle. Having the equations explained in chapter two that can be rearranged in:

$$\begin{cases} mu\dot{\beta} = Y_\beta \beta + \left(Y_\rho - mu^2\right)\rho + Y_\delta \delta \\ J_z u\dot{\rho} = N_\beta \beta + N_\rho \rho + N_\delta \delta \end{cases} \tag{5.1}$$

Where ρ is the ratio between $\dot{\psi}$ and u

Stability derivative	Formulation	Definition
Damping in sideslip	$Y_\beta = C_1 + C_2$	$Y_\beta = \dfrac{\partial Y}{\partial \beta}$
Lateral force/Yaw coupling	$Y_{\dot{\psi}} = \dfrac{(a_1 C_1 - a_2 C_2)}{u}$	$Y_{\dot{\psi}} = \dfrac{\partial Y}{\partial \dot{\psi}}$
Control Force	$Y_\delta = -C_1$	$Y_\delta = \dfrac{\partial Y}{\partial \delta}$
Direction stability	$N_\beta = a_1 C_1 + a_2 C_2$	$N_\beta = \dfrac{\partial N}{\partial \beta}$
Yaw damping	$N_{\dot{\psi}} = (a_1^2 C_1 - a_2^2 C_2)/u$	$N_{\dot{\psi}} = \dfrac{\partial N}{\partial \dot{\psi}}$
Control Moment	$N_\delta = -a_1 C_1$	$N_\delta = \dfrac{\partial N}{\partial \delta}$

Table 5-2 Kalman filter parameters

The vehicle inputs necessary to set the car model are:

- Mass;
- Moment of inertia;
- Wheelbase;
- Mass distribution on the axles;
- Front and rear cornering stiffness.

Mass, mass distribution and wheelbase are easily measurable.

Although the software developed in Stellantis can determinate the inertia by analyzing a series of maneuvers, the moment of inertia has been calculated with the geometric formula:

$$J_z = M_{front}a_1^2 + M_{rear}a_2^2$$

Where M_{front} and M_{rear} are the masses respectively considered in the front and rear axels.

5.2 Procedure for estimating the sideslip angle.

This paragraph will explain the procedure that was used to formulate an algorithm that estimates the sideslip angle. As seen in the previous paragraph, the necessary inputs to the model are:

- Mass;
- Moment of inertia;
- Wheelbase;
- Mass distribution on the axles;
- Front and rear cornering stiffness.

The front and rear cornering stiffness must therefore be calculated. One methodology would be to use Stellantis software, that notes the pneumatics and lateral acceleration intervals for that vehicle, return the value of the cornering stiffness. A simplified scheme is shown in the Figure 5-2. However, this method is not applicable in all conditions. In fact, if we replace the tires with tires of a different type, the model could be affected and the results would not be so faithful.

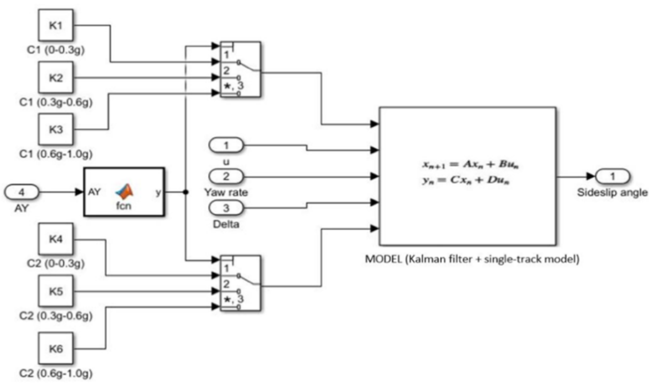

Figure 5-2 Simulink block Steady state reference maneuver with three values of cornering stiffnesses depending on the lateral acceleration

At this point it is therefore necessary to find a methodology that allows to calculate the cornering stiffness in any condition. The steps to follow are the following:

1. Sideslip angle estimation with kinematic model in steady state standard maneuvers;
2. Slip angles estimation;
3. Forces interpolation;
4. Cornering stiffnesses estimation.

A Simulink scheme is shown below which summarizes all the steps to be performed.

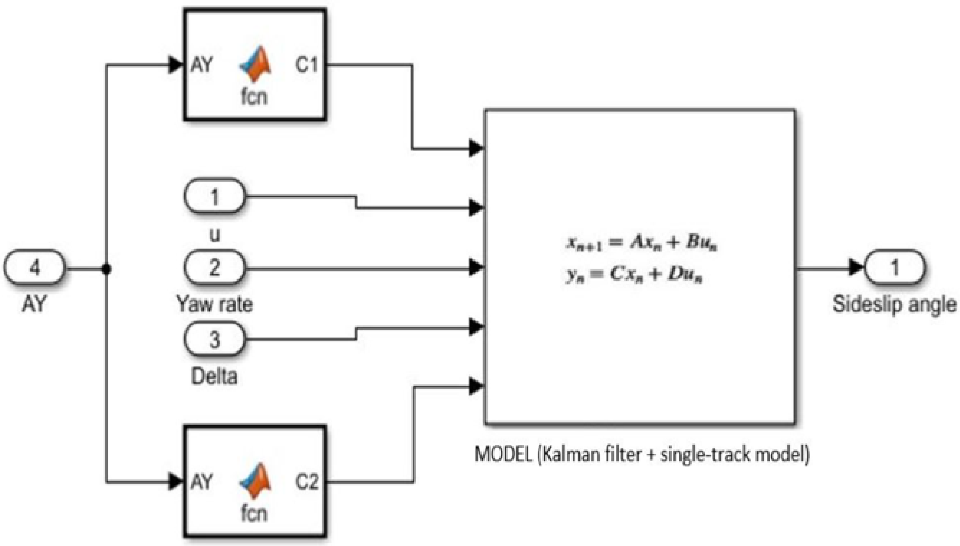

Figure 5-3 Simulink block Steady state reference maneuver with two functions of cornering stiffnesses

5.2.1 Initial operations for using signals.

The signals obtained by the acquisition are not ready to be used, some post-processing steps must be done; Stellantis exploits a self-made software for the signal analysis, which is able to make some basic operations. This software is good at compensating some physical limits of the measures, in particular:

- Sensors position;
- Signal shifting.

Indeed, sensors are not positioned in the car center of gravity; this means that the measured values can be affected by kinematic and geometrical inaccuracy.

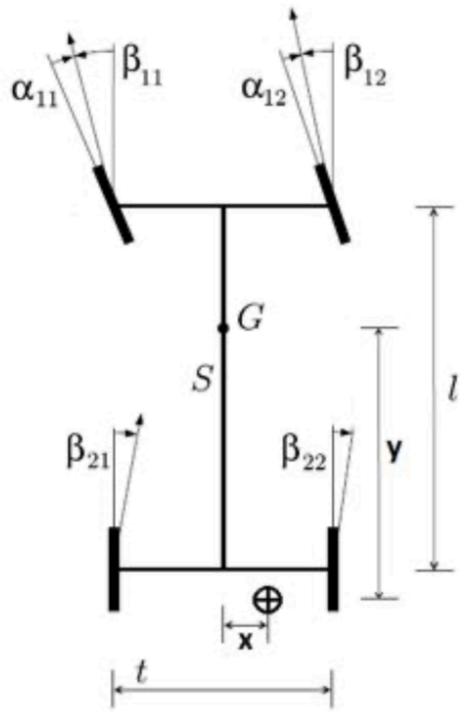

Figure 5-4 Typical optical sensor position for tests

The software uses the sensors coordinates to compensate the geometrical errors. Then, for example, it employs other measured signals like the angular unsprang mass position to rectify the lateral acceleration. Although the correction is not so relevant for the other signals, it is for the sideslip angle. The geometrical correction is more important than the kinematic, indeed the last one can be neglected. The procedure is analogue to the one used to pass from the tyre VSA to the center of gravity one.

About the signal shifting, the measures can be subject to a drift from the beginning to the end of the maneuver; for example, even though the steering wheel is equal to 0 at the beginning and at the end of the maneuver, VSA could start from 0 and finish with a different value. This phenomenon is compensated by a linear correction, which puts the VSA (such as other signals) to zero. Another operation to do is the measures offsetting: it is necessary because, although the accuracy of the sensor is not influenced by the mounting process, the absolute measured values are. For this reason, all the maneuvers start from a neutral zero-condition:

$$\begin{cases} a_x = a_y = \dot{\psi} = \delta = 0 \\ u = costant \end{cases}$$

So that it's easy to identify a Δt for the offset operation. It's important to convert the physical quantities to the right unities of measurement. This is not a problem for the Artificial Neural Network because the determination of the links between different parameters is independent on multiplicator factors. On the contrary, Kalman filter-based estimator employs a specific single-track model which needs the right units. The steering wheel angle must be transposed to the wheel angles so that it must be divided for the medium steering rate. After this post-process, the measures might be used, but in the case of significant noise, an additional work is useful and recommended. There are some unpredictable factors which can change the noise intensity; Furthermore, sometimes some filters are applied to clean up the signals:

- Low-pass filter;
- Moving-mean filter.

The interesting frequencies for the longitudinal and the lateral dynamics are the lower ones; it's really hard to exceed the 4 Hz in these conditions and, however, over 2÷2.5 Hz the behavior is negligible for the characterization of the vehicle dynamic. In the first acquisition phase the signals are already filtered over 10 Hz, by the software used; due to the noise, if it was useful the operation was repeated till 5 Hz or lower in case of necessity. Obviously, this operation must need a final check to verify the coherence of the values: loss of signal information must be avoided. In case of strong noise which produces rapid fluctuations around the right value, a moving-mean filter was applied, limiting this problem.

5.2.2 Definition of the starting point and ending point of the test

After having transferred all the data acquired by the sensors to the center of gravity, it is necessary to define the starting point and the ending point of the test in question. In the case of the ramp steer test, the starting point SP is the point, in terms of time, for which the driver begins to steer while the ending point EP is the moment in which the driver stops. It is possible to schematize what has been said through the figure:

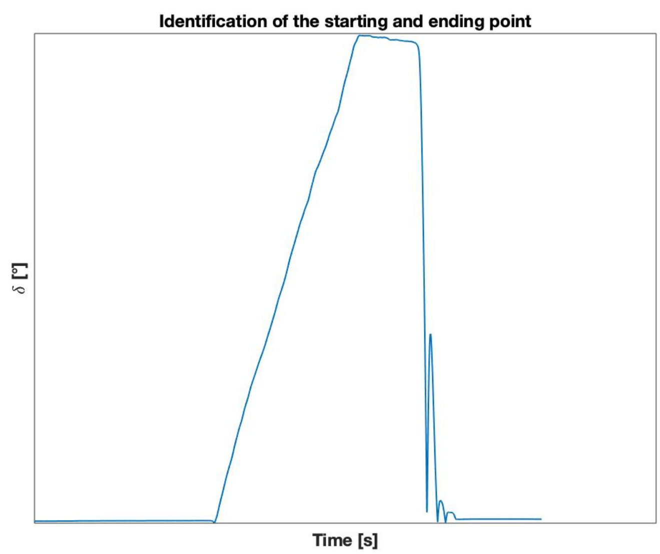

Figure 5-5 the steering wheel angle for a test of ramp steer with $u = 100\ km / h$

The starting and ending point were calculated by evaluating the steering wheel angle variation. The starting point was identified if, in a discrete model, the variation of the steering wheel was greater than a minimum value. Instead, the ending point was evaluated when the variation of the steering wheel angle after the starting point SP was reduced to a certain value.

Having calculated the starting point and ending point values, it was possible to filter the sensor information only between the two values.

5.2.3 Sideslip and slip angle estimation with kinematic model in steady state standard maneuvers

Starting from the kinematic model, as already explained the system can be represented by two equations:

$$\begin{cases} a_x = (\dot{u} - \dot{\psi}\, v) \\ a_y = (\dot{v} + \dot{\psi}\, u) \end{cases} \tag{5.2}$$

Once, the lateral speed is computed, the sideslip angle can be estimated:

$$\beta = arctg\left(\frac{u}{v}\right) \tag{5.3}$$

Having a discretized signal, the speed can be calculated as:

$$v_{k+1} = v_k - T_s\dot{\psi}u_k + T_s {a_y}_k \tag{5.4}$$

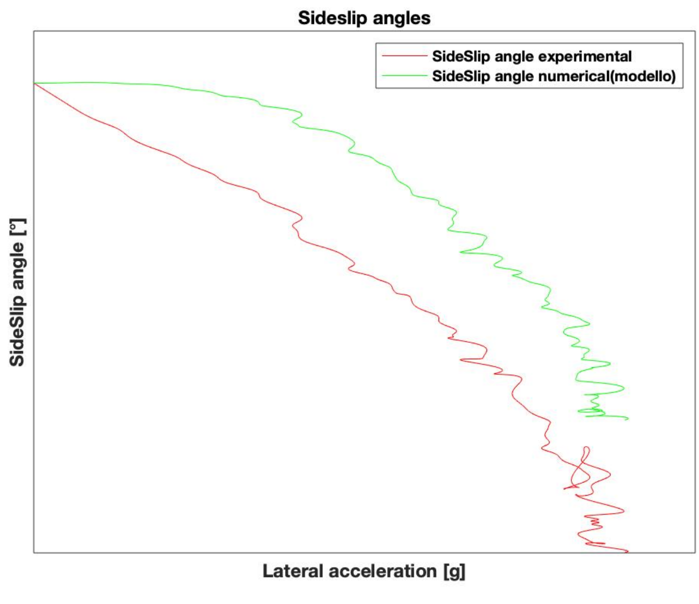

Figure 5-6 Sideslip angle estimation with kinematic model in steady state standard maneuvers

The sideslip angle estimation by the kinematic model might generate several problems, especially if the signals are not with accurate off-set. In the first part an opposite sign of the angle might be estimated in some circumstances.

Considering that in standard conditions:

$$u \gg v\,; u \gg a_i|\dot{\psi}|\,; u \gg |\dot{\psi}|\frac{t_i}{2}$$

Where t_i is the wheel track.

It is possible to obtain that tyres of the same axle have almost same sideslip angle, β_1 for the front and β_2 for the rear. The steering system is usually build to have similar front steering angles $(\delta_{i1} \simeq \delta_{i2}) = \delta_i$, especially at high speed. In this way the slip angles estimation can be computed, through the equations:

$$\alpha_1 = \delta_1 - \beta - \left(\frac{\dot{\psi}}{u}\right) a_1 \tag{5.5}$$

$$\alpha_2 = -\beta + \left(\frac{\dot{\psi}}{u}\right) a_2 \tag{5.6}$$

Where:

$$\alpha_{11} \cong \alpha_{12}\,; \;\; \alpha_{21} \cong \alpha_{22}$$

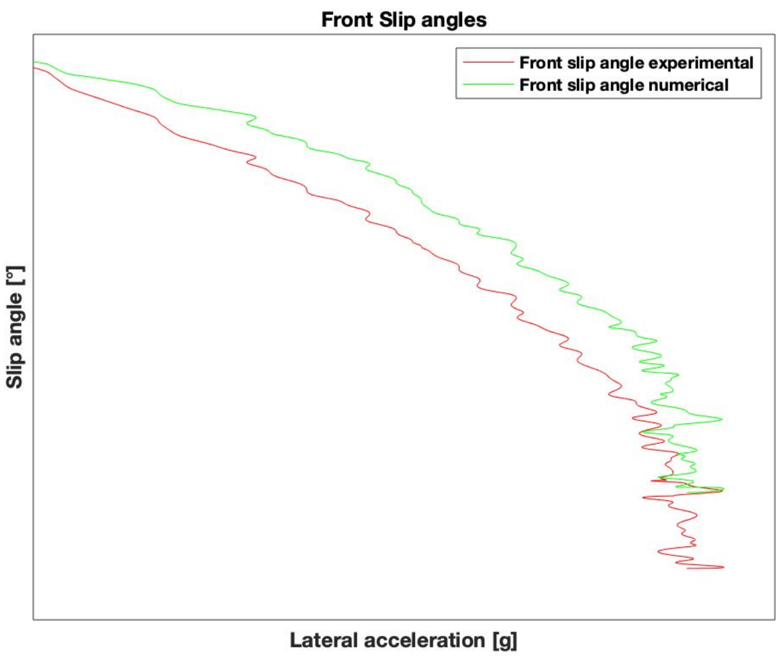

Figure 5-7 Front slip angle estimation with kinematic model in steady state standard maneuvers

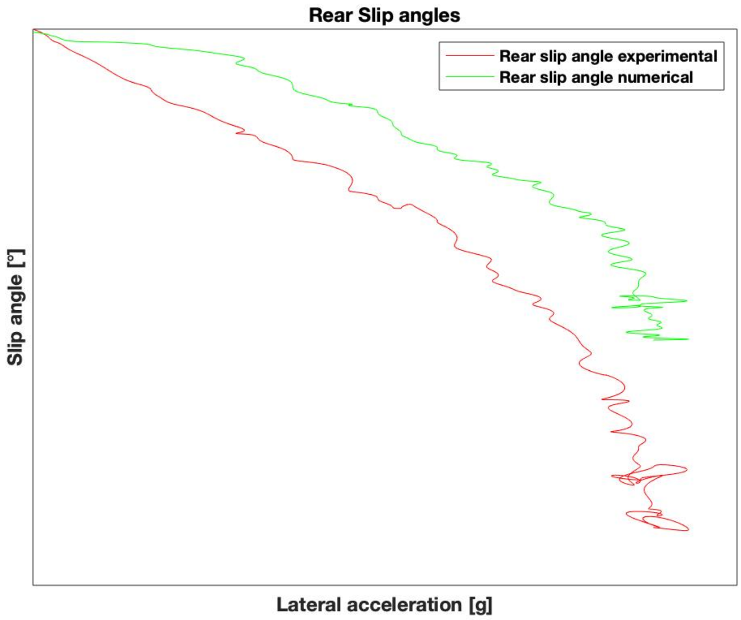

Figure 5-8 Rear slip angle estimation with kinematic model in steady state standard maneuvers

The result of the slip angles, as shown in the *Figure 5-8* and *Figure 5-7*, is not optimal due to the sideslip angle error.

5.2.4 Forces interpolation and cornering stiffnesses estimation

The accelerometer on the vehicle allows you to evaluate the three components of the vehicle's acceleration instant by instant.

The acceleration data provided by the sensor must be valued to the center of gravity using the following relationship:

$$a_p = a_g + \dot{\vec{w}} \times \vec{r} + \vec{w} \times (\vec{w} \times \vec{r}) \tag{5.7}$$

It is therefore possible to calculate the value of the lateral forces applied to the vehicle.

Moreover, starting from the equilibrium equations, neglecting the longitudinal vehicle dynamic and considering the lateral force of the front tyres as the sum of the left and right tyre lateral force, $Fy_1 = Fy_{11} + Fy_{12}$, as well as for the rear $Fy_2 = Fy_{21} + Fy_{22}$, remembering that this is possible only due to the assumption of the front tyres work with (almost) equal sideslip angles as well as for the rear:

$$\begin{cases} m\, a_y = F_{y_1} + F_{y_2} \\ J_z \ddot{\psi} = F_{y_1} a_1 - F_{y_2} a_2 \end{cases} \tag{5.8}$$

Considering the yaw acceleration $\ddot{\psi}$, in this type of maneuver it is practically null and solving for F_{y1} and F_{y2}:

$$\begin{cases} F_{y_1} = \left(\frac{ma_y}{a_1+a_2}\right) a_2 \\ F_{y_2} = \left(\frac{ma_y}{a_1+a_2}\right) a_1 \end{cases} \tag{5.9}$$

Remembering that this procedure is made in standard steady state maneuvers, usually six steady state maneuvers are used, three for each side for statistical robustness. Furthermore, referring to the bicycle model, the forces interpolation through the Pacejka model, estimating the parameters B,C,D and E for the entire front axle and for the entire rear axle. One set of parameters for the front, considering it as a single tyre and one set of parameters for the rear, considering it as a single tyre:

$$Y = D\, sin\left[C\, arctang\left(Bx - E\big(Bx - arctang(Bx)\big)\right)\right] \tag{5.10}$$

To calculate the unknown parameters, the lsqcurvefit command was used; The lsqcurvefit command will be detailed in the paragraph 5.3.1. Moreover, forces at high values of slip angles are estimated, however at the rear, having available data mainly up to 2° of slip angle, the reliability decreases as the curves go further this threshold, especially for the rear due to the fact that the car is an understeering vehicle and it could not usually reach these values of rear slip angle. To improve the model and minimize the error linked to the rear lateral force, it is necessary to perform special tests, designed to evaluate in more detail the achievement of the rear axle saturation.

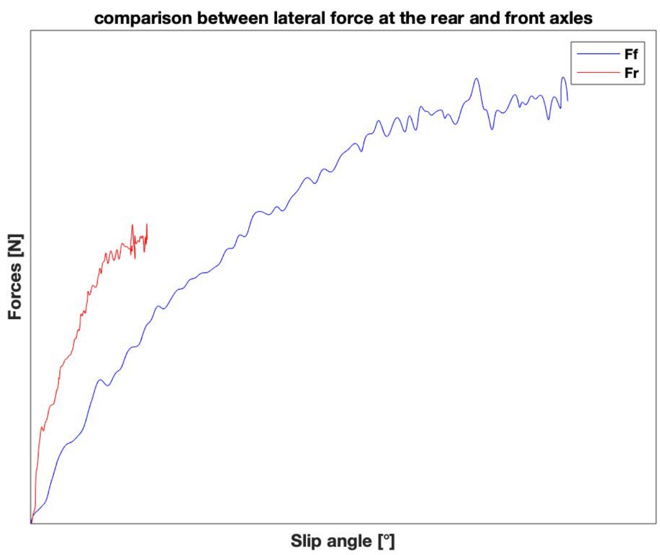

Figure 5-9 Front and rear forces experimental data

The forces shown in the *Figure 5-9* are the lateral forces on the axles that the car during the test.

A model that considers relaxation lengths should be implemented in the algorithm. This addition would increase the number of states from two to four. A Kalman filter based on a dynamic system of double size should therefore be implemented to consider the delay introduced by the tires. In the first instance this function has not been implemented but it is necessary to consider it for future development of the project.

The resulting cornering stiffnesses estimation are made considering the ratio between lateral force and slip angle of the respective axes.:

$$C_\alpha = \left(\frac{\Delta F_y}{\Delta \alpha}\right) \tag{5.11}$$

The cornering stiffness resulting are:

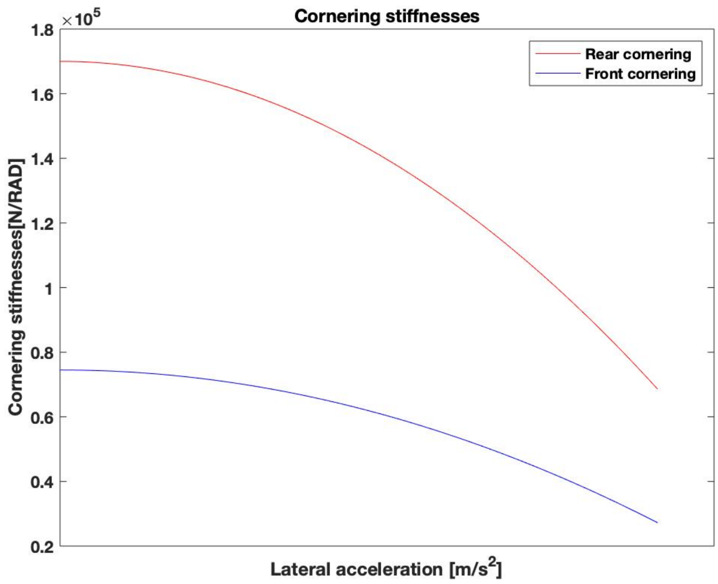

Figure 5-10 Front and rear cornering stiffnesses estimation

5.2.5 Results

After having estimated the sideslip stiffness values, it is possible to calculate the parameters in Table 5-2

By discretizing equation (5.1) we obtain:

$$\begin{cases} \dfrac{\beta_{k+1}-\beta_k}{Ts} = \dfrac{Y_\beta}{mu}\beta_k + \dfrac{Y_{\dot\psi}-mu}{mu}\dot\psi + \dfrac{Y_\delta\delta}{mu} \rightarrow \beta_{k+1} = \left(\dfrac{T_sY_\beta}{mu}+1\right)\beta_k + T_s\left(\dfrac{Y_{\dot\psi}-mu}{mu}\right)\dot\psi + \dfrac{T_sY_\delta}{mu}\,\delta_k \\ \dfrac{\dot\psi_{k+1}-\dot\psi_k}{Ts} = \dfrac{N_\beta}{J_z}\beta_k + \dfrac{N_{\dot\psi}}{J_z}\dot\psi + \dfrac{N_\delta\delta}{J_z} \rightarrow \dot\psi_{k+1} = \left(\dfrac{T_sN_\beta}{J_z}\right)\beta_k + \left(\dfrac{T_sN_{\dot\psi}}{J_z}+1\right)\dot\psi_k + \dfrac{T_sN_\delta}{J_z}\,\delta_k \end{cases}$$

Therefore:

$$A = \left(\frac{T_sY_\beta}{mu}+1\right)\beta_k \tag{5.12}$$

$$B = \begin{vmatrix} T_s\left(\frac{Y_{\dot\psi}-mu}{mu}\right) \\ \frac{T_sY_\delta}{mu} \end{vmatrix} \tag{5.13}$$

$$C = \left(\frac{T_sN_\beta}{J_z}\right) \tag{5.14}$$

$$D = \begin{vmatrix} \left(\frac{T_sN_{\dot\psi}}{Jz}+1\right) \\ \frac{T_sN_\delta}{Jz} \end{vmatrix} \tag{5.15}$$

By applying the Kalman filter with the matrices defined above, the sideslip angle is obtained.

For this application, the covariance matrices have been set equal to diagonal matrices of value 0,1. This value was chosen based on experience. However, it is possible to search for an optimization regarding this parameter. This aspect will be analyzed in the following chapters.

The results of the Kalman filter applied to the dynamic model for calculating the sideslip angle are the following:

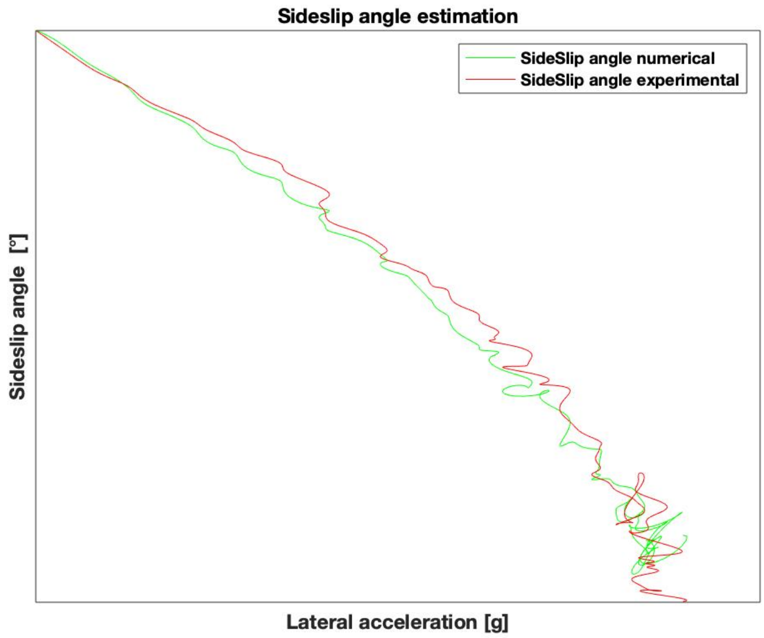

Figure 5-11 Sideslip angle estimation with the application of the Kalman filter to the vehicle dynamic model in steady state standard maneuvers

Comparing *Figure 5-11* with figure *Figure 5-6* we notice how the model that uses KF returns values that are closer to real data than the model that uses only the kinematic model. It should be noted that once the correct sideslip angle has been calculated, it is possible to recalculate the other parameters to have a better estimate. The results are as follows:

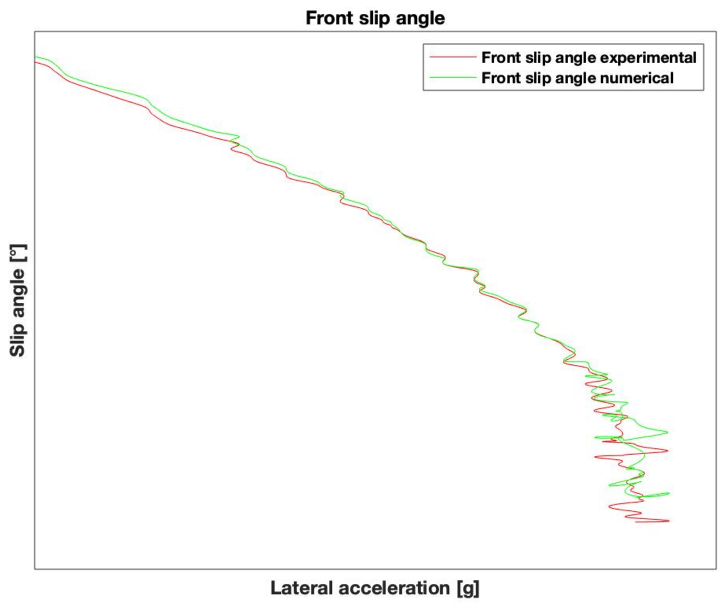

Figure 5-12 Front slip angle estimation with the application of the Kalman filter to the vehicle dynamic model in steady state standard maneuvers

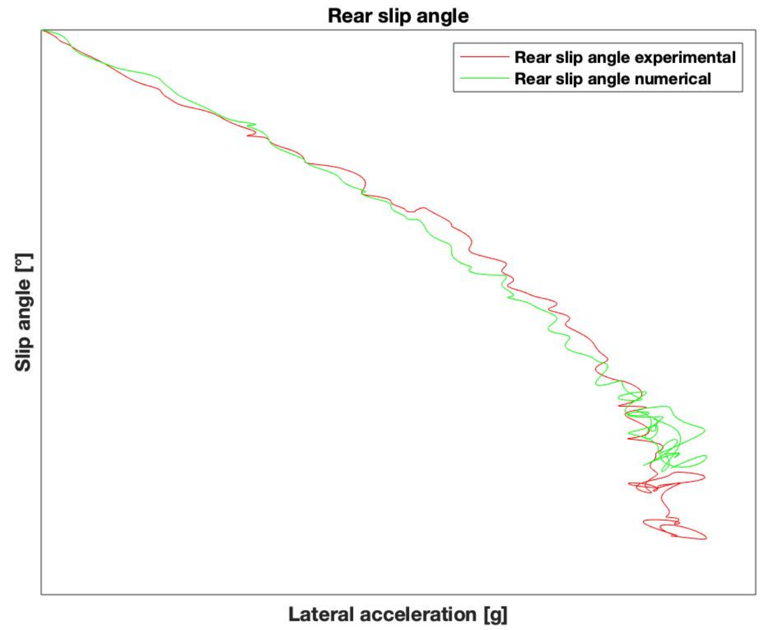

Figure 5-13 Rear slip angle estimation with the application of the Kalman filter to the vehicle dynamic model in steady state standard maneuvers

Once a more correct value of the sideslip angle has been obtained, through the vehicle dynamics equations it is possible to have a more efficient estimate of the cornering stiffnesses.

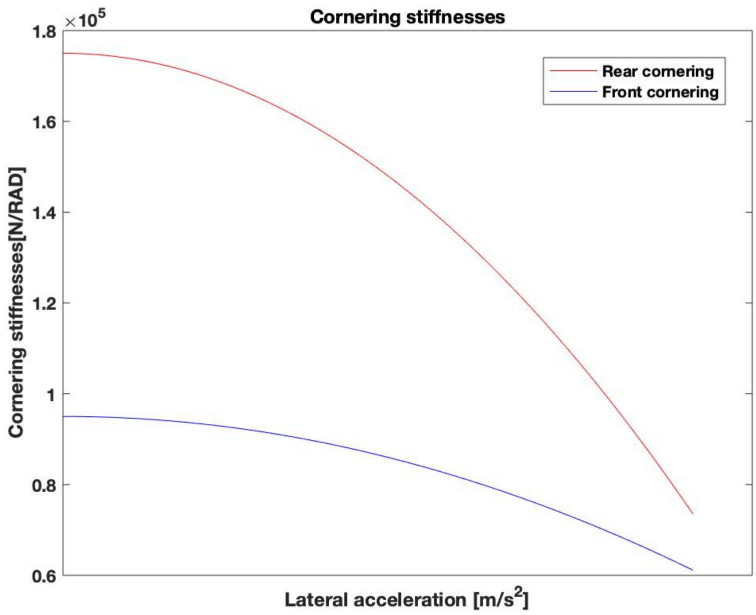

Figure 5-14 Front and rear cornering stiffnesses estimate after application of Kalman filter

From the *Figure 5-11* it is immediately visible the net improvement obtained in terms of estimating the sideslip angle.

In order to have an objective measure of the estimation error and the improvement obtained by passing from the estimation with the kinematic model only to the model that uses the Kalman filter, the parameters of MAE and RMSE errors described in paragraph 4.6 are used.

The error obtained for the above test, in terms of MAE before the application of the filter was 3.52°, while in terms of RMSE it was 4.01°. Through the application of the filter the MAE and the RMSE are drastically reduced obtaining values of 0.15° and respectively 0.181°. The figure *Figure 5-15* shows the error trend as the lateral acceleration varies.

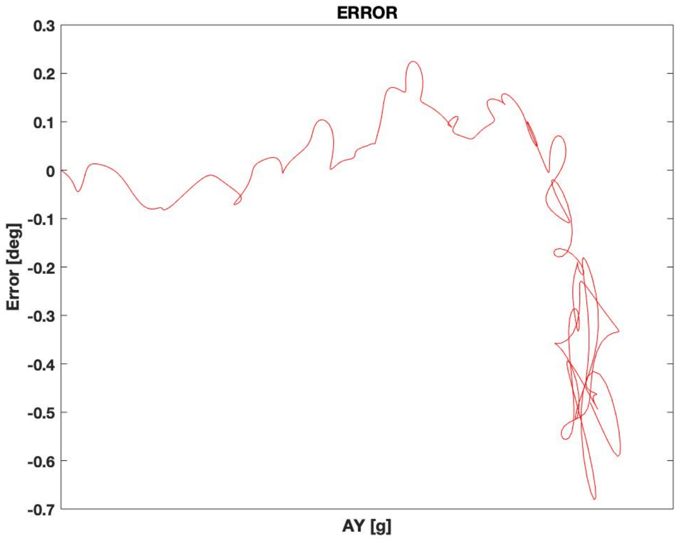

Figure 5-15 Error when acceleration varies due to ramp steer test.

In order to have a clear and complete view of the whole process which, from the inputs leads to the estimate of the sideslip angle of the car, an overall flowchart of the model is shown in the *Figure 5-16*.

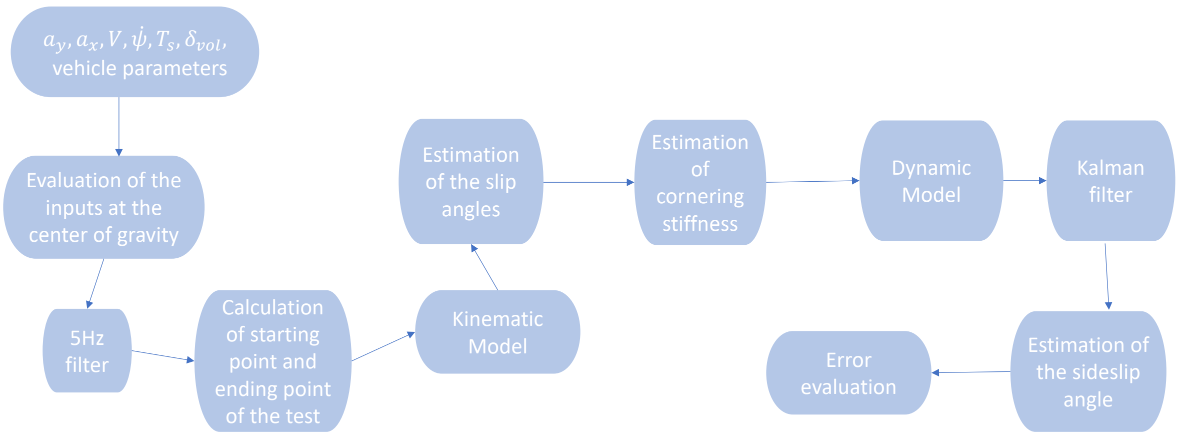

Figure 5-16 Flow chart of the Matlab model for steady-state test

5.2.6 Understeer characteristic

The **understeer characteristic** [27] is a stationary characteristic which relates the difference between the steering angle and the kinematic steering angle ($\delta - \delta_0$) and the lateral acceleration (a_y). The kinematic steering angle is the ratio between the wheelbase of the car used and the radius of the trajectory.

$$\delta_o = \frac{l}{R} \tag{5.16}$$

$$R = \frac{a_y}{\dot{\psi}^2} \tag{5.17}$$

From the understeer characteristic it is also possible to derive the understeer gradient (K_{us}), intended as the angular coefficient of the initial straight section of the characteristic.

From *Figure 2-3* of the single-track vehicle model, it is possible to derive the geometric relationships resulting from a condition of stationary motion:

$$\delta - \delta_0 = \alpha_F - \alpha_R \tag{5.18}$$

$$a_y \cong a_{y_F} \cong a_{y_R} \tag{5.18}$$

$$Fy_F = m_F \cdot a_y = Cy_F \cdot \alpha_F \tag{5.19}$$

$$F_{y_R} = m_R \cdot a_y = C_{y_R} \cdot \alpha_R \tag{5.20}$$

Combining the equations:

$$\delta - \delta_0 = (m_F C_{yF} - m_R C_{yR}) \cdot a_y = K_{US} \cdot a_y \tag{5.21}$$

Depending on the value of K_{us} the vehicle can be

- **Neutral Steer**, if $m_F / C_{\alpha_F} = m_R / C_{\alpha_R} \rightarrow K_{us} = 0 \rightarrow \alpha_F = \alpha_R$; On a curve with a constant radius of curvature, no change in the steering angle is required as the forward speed varies. It is equal to the required steering angle in kinematic steering conditions. Neutral steering corresponds to a balance on the vehicle such that the centrifugal force generates, as the forward speed varies, identical increases in the slip angles at the front and rear.
- **Understeer**, if $m_F / C_{\alpha_F} > m_R / C_{\alpha_R} \rightarrow K_{us} > 0 \rightarrow \alpha_F > \alpha_R$: on a curve with a constant radius of curvature, as the forward speed increases, an increase in the steering angle is required proportional to the increase in centripetal acceleration according to the K factor, to keep the vehicle on track. Understeer corresponds to

the condition that lateral acceleration requires an increase in the slip angle which is greater on the front wheels than on the rear ones. For this reason, in order for the front wheels to be able to develop the lateral forces necessary to keep the vehicle in trajectory, it is necessary that they take on a steering angle greater than that required in kinematic steering conditions.

- **Oversteer**, if $m_F/C_{\alpha_F} < m_R/C_{\alpha_R} \rightarrow K_{us} < 0 \rightarrow \alpha_F < \alpha_R$: on a curve with a constant radius of curvature, as the forward speed increases, a decrease in the steering angle proportional to the increase in centripetal acceleration according to the K factor, to keep the vehicle on the path. Oversteer corresponds to the condition that lateral acceleration requires an increase in the slip angle which is greater on the rear wheels than on the front ones. For this reason, in order for the front wheels to be able to develop the lateral forces necessary to keep the vehicle in the trajectory (avoiding to make it close the trajectory) it is necessary that they take on a lower steering angle than that required in kinematic steering conditions.

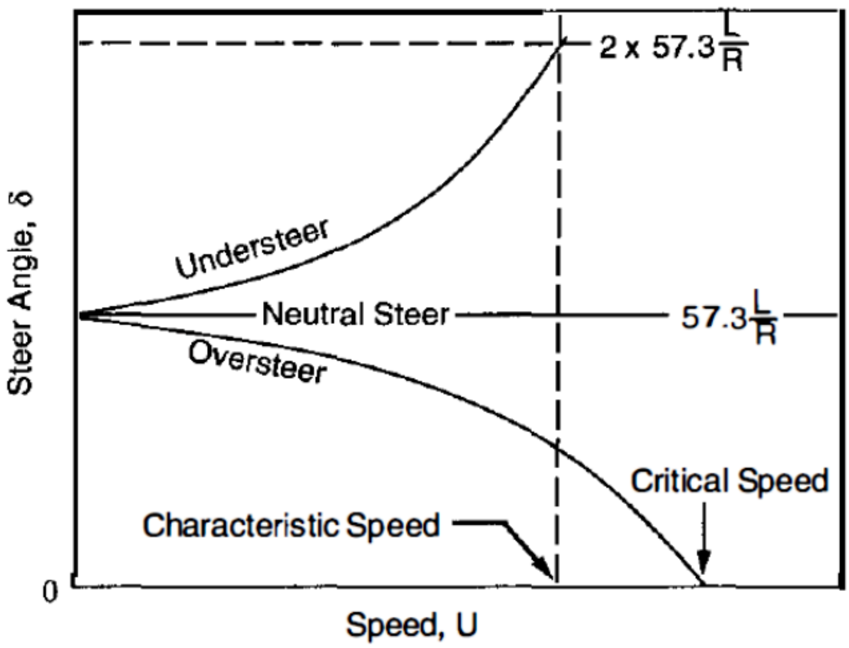

Figure 5-17 Steering angle required as a function of forward speed

For an understeer vehicle, the characteristic speed is defined as the speed at which the required steering angle is double the kinematic steering angle, whatever the radius of curvature R:

$$V_{car} = \sqrt{57.3\ lg/K_{us}} \tag{5.22}$$

For an oversteer vehicle, however, the critical speed is defined as the speed at which the required steering angle is zero and the vehicle is in an unstable operating condition:

$$V_{car} = \sqrt{-57.3\ lg/K_{us}} \tag{5.23}$$

In the test in question, the steering curve is as follows:

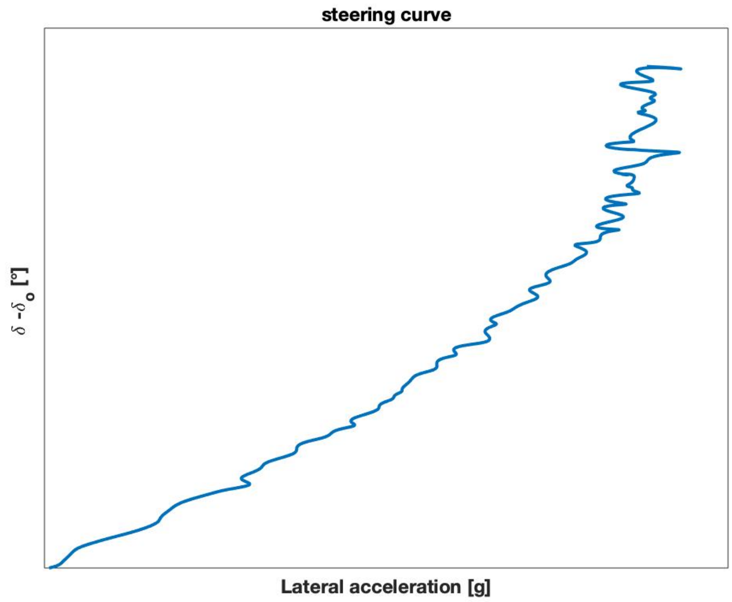

Figure 5-18 Steering curve

Because K_{us} is positive then the vehicle is understeering.

The sideslip characteristic is a stationary characteristic that relates the difference between the sideslip angle and the kinematic sideslip angle ($\beta - \beta_0$) and the lateral acceleration (ay). The kinematic sideslip angle is the ratio between the rear half-step of the car used (b) and the radius of the trajectory $\beta_o = \frac{b}{R}$

From the sideslip characteristic it is also possible to derive the sideslip gradient (K_β), intended as the angular coefficient of the initial straight section of the characteristic. From *Figure 2-3* of the single-track vehicle model, it is possible to derive the geometric relationships resulting from a condition of stationary motion:

$$\beta - \beta_0 = -\alpha_R \tag{5.24}$$

Combining the equations:

$$\beta - \beta_0 = -\left(\frac{m_r}{C_{y_r}}\right) \cdot ay = -K_\beta \cdot ay \tag{5.25}$$

5.3 Command lsqcurvefit e movmean

This paragraph explains how the lsqcurvefit command and the movmean command work. These commands were necessary for the generation of the algorithm for estimating the sideslip angle.

5.3.1 Command lsqcurvefit

This command determines the unknown parameters by finding the curve that minimizes the sum of the squares of the distances between the observed data and those of the curve that represents the function itself. In order to operate it requires:

- A fit function in which there are unknown parameters to be determined;
- Data to perform the fit;
- An initial value X_0 containing the values of the first attempt parameters from which to start the iteration;

The function to be minimized (respect to X) is the following:

$$F(X,k,r) = \sum_{i=1}^{n}(y(X,k_i) - r_i)^2 \tag{5.26}$$

Where:

- y is the function chosen for the fit;
- k_i is the independent variable;
- n is the number of samples;
- r_i is the value to be fit;
- X is the vector containing the values of the coefficients to be determined.

The figure shows how the lsqcurvefit command works for force F_{y_1}:

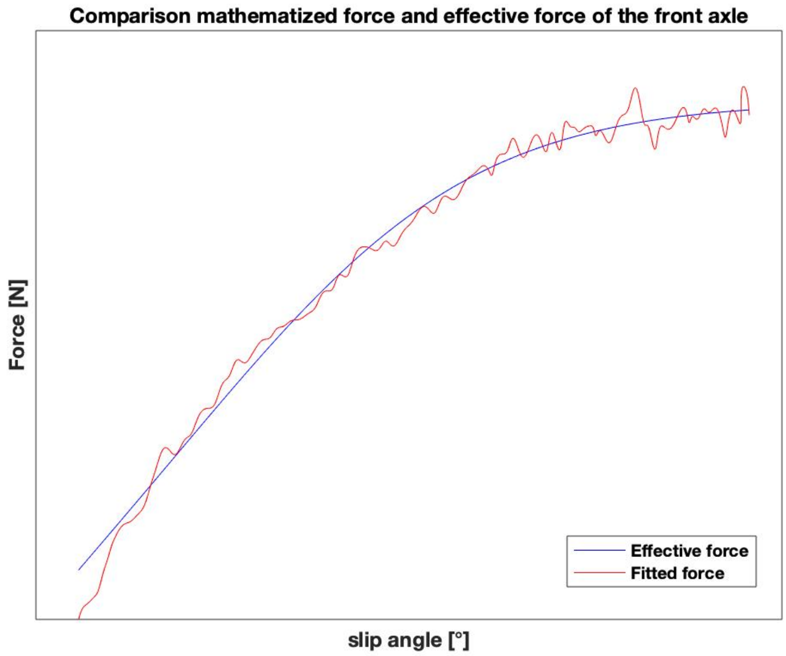

Figure 5-19 example of the operation of the lsqcurvefit command applied to the front lateral force

5.3.2 Command movmean

Movmean is a Matlab function that allows you to make a moving average of a discrete signal. Once the size of the window has been defined, it moves and makes the arithmetic average within the window itself, after which, the window moves and continues to average for every i-th instant. An example is the following:

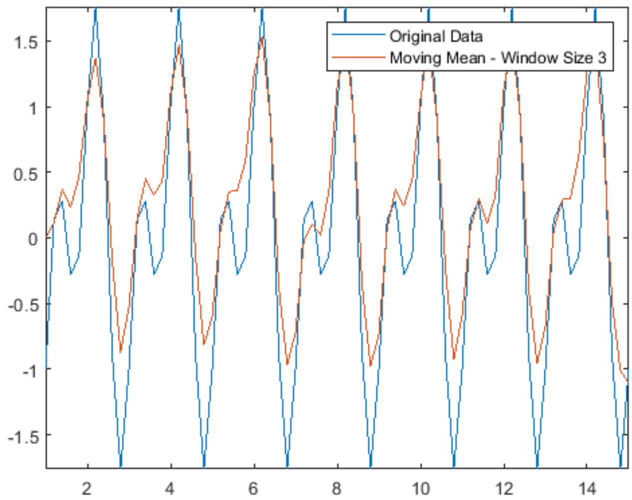

Figure 5-20 Example of the operation of the movmean command

5.4 Choice of the values of the covariance matrix of the model and of the measure

Paragraph 5.2.5 shows the results achieved by imposing a diagonal matrix with values of 0.1 as a covariance matrix. These values were defined by experience in the various tests. As seen in paragraph 3.2, the covariance matrices indicate the level of reliability of the model and of the measure. This paragraph analyzes in detail the methodology with which it is possible to calculate the values of the covariance matrices.

5.4.1 Choice of the values of the covariance matrix of the measure

The matrix R is the covariance matrix of the measure and quantifies the variance of the error linked to the measure. It is possible to evaluate the variation of the error linked to the instrumentation by evaluating the noise generated by the instrumentation by providing it with a constant signal. In the case in question, the sensor must acquire a stationary test with constant sideslip angle.

However, the evaluation of the noise does not allow to obtain an objective value to be assigned to R, however by comparing the noise of the model with the noise of the measurement it is possible to have a reliability ratio and thus obtain the values required.

One method to evaluate sensor-related noise would be to compare this with one that has a bandwidth of at least one order of magnitude greater.

This process is also used for the **calibration** of measuring instruments.

5.4.2 Choice of the values of the covariance matrix of the model

Much more complicated is the choice of the covariance matrix for the model. In this paragraph the Kalman filter and in particular the noise linked to the model are examined in depth [15] [16].

The concept of covariance is, as we have seen, linked to noise. It is necessary to distinguish the noise into two categories:

White noise: if RV (t_1), vector of stochastic values, is always different from RV (t_n) with e $n \in [1, N]$

Colored noise: if the above condition is not respected.

The system that has been analyzed in this particular case is a linear-discrete time system.

$$x_k = F_{k-1}x_{k-1} + G_{k-1}u_{k-1} + w_{k-1} \tag{5.27}$$

where u_k is a known input and w_k is Gaussian zero-mean white noise with covariance Q_k. How does the mean of the state x_k change with time? If we take the expected value of both sides of Equation (6.1) we obtain:

$$\overline{x_k} = F_{k-1}\overline{x_{k-1}} + G_{k-1}u_{k-1} \tag{5.28}$$

By combining the equations (6.1) and (6.2) to obtain:

$$(x_k - \overline{x_k})\,(\ldots)^T = F_{k-1}\,(x_{k-1} - \overline{x_{k-1}})\,w_{k-1}^T + w_{k-1}(x_{k-1} - \overline{x_{k-1}})^T F_{k-1}^T \tag{5.29}$$

We therefore obtain the covariance of x_k as the expected value of the above expression. Since $(\mathrm{x}_{\mathrm{k}-1} - \overline{\mathrm{x}_{\mathrm{k}-1}})$ is uncorrelated with w_{k-1}, we obtain:

$$P_k = F_{k-1}P_{k-1}\,F_{k-1}^T + Q_{k-1} \tag{5.30}$$

This is called a discrete-time Lyapunov equation, or a Stein equation [17]. It is interesting to consider the conditions under which the discrete-time Lyapunov equation has a steady-state solution. That is, suppose that $F_k = F$ is a constant, and $Q_k = Q$ is a constant. Then we have the following theorem, whose proof can be found in [31].

Therefore, for the calculation of the covariance matrix linked to the model of the sideslip angle calculation it is therefore necessary to make a first analysis that allows us, starting from the average values, to obtain w_k.

Starting from the average relationship:

$$\frac{\beta_{k+1} - \beta_k}{Ts} = \frac{Y_\beta}{mu}\beta_k + \frac{Y_{\dot\psi} - mu}{mu}\,\dot\psi + \frac{Y_\delta \delta}{mu} \rightarrow \beta_{k+1} = \left(\frac{T_s Y_\beta}{mu} + 1\right)\beta_k + T_s\left(\frac{Y_{\dot\psi} - mu}{mu}\right)\dot\psi + \frac{T_s Y_\delta}{mu}\,\delta_k$$

Therefore, it is possible to develop the Lyapunov equation to obtain the covariance matrix of the model itself. There are some Matlab functions such as X = dylap (A, Q) which solves the equation seen above having known the noise related to the model.

5.5 Transient reference maneuver

The sideslip angle estimation model has provided excellent results as shown in the paragraph 5.2.5 .

However, for a more complete analysis of the vehicle's dynamic performance, it is also necessary to test it in standardized transient tests such as sweep tests. As treated by the ISO standards, this test is performed at 120 km/h by changing the lateral acceleration range: 0.3g-0.5g- 0.7g

The results obtained for the 0.3g test will be shown below; The model built for the steady-state ramp steer test case still remains valid although the calculation of the SP and EP must be modified.

The vehicle sensor allows to obtain the following information:

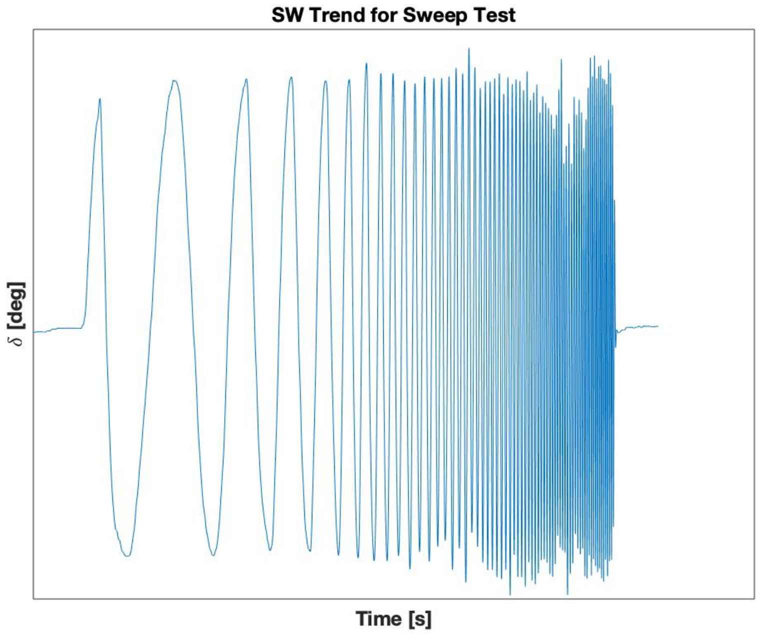

Figure 5-21 Steering wheel angle for sweep test u=120km/h, ay=0,3g

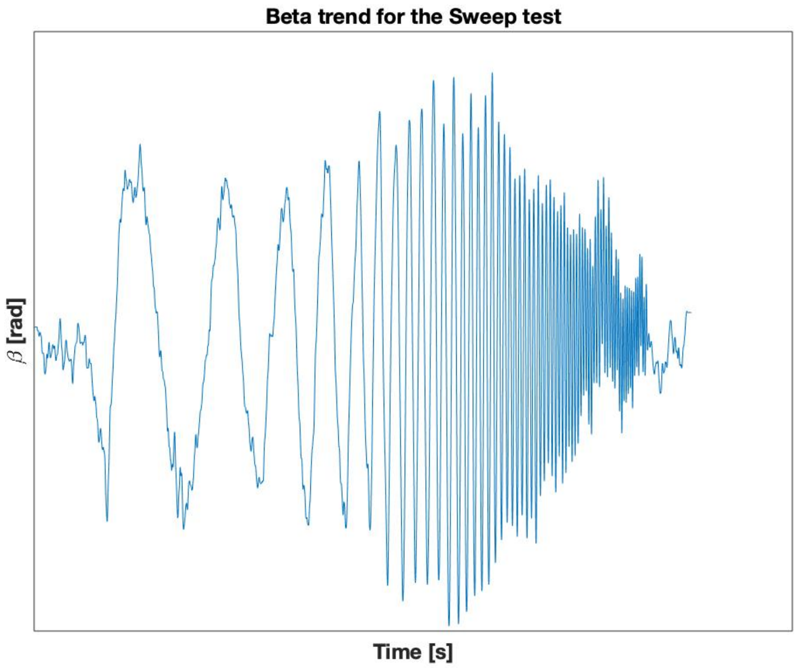

Figure 5-22 Sideslip angle for sweep test u=120km/h, ay=0,3g

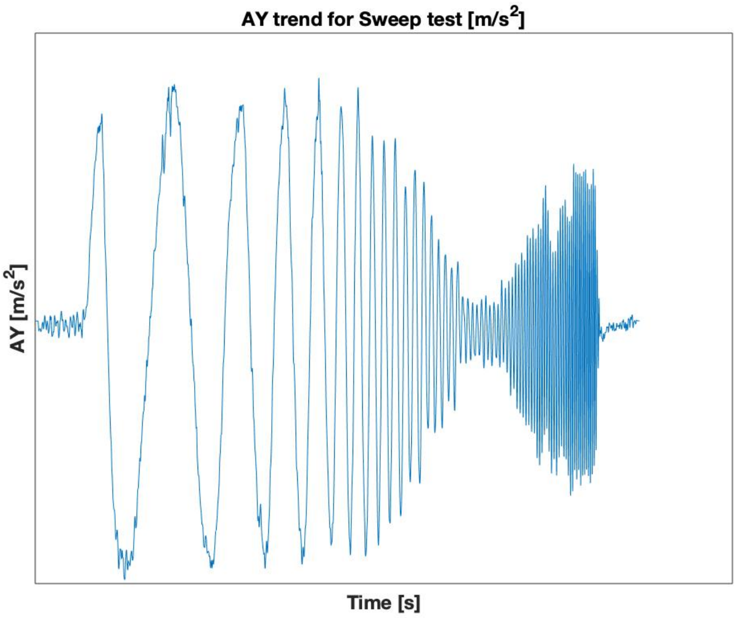

Figure 5-23 Lateral acceleration for sweep test u=120km/h, ay=0,3g

The kinematic model that allows a first estimate of the sideslip angle and therefore of the sideslip angle, according to the paragraph formulations 2.3.1, returns the following results:

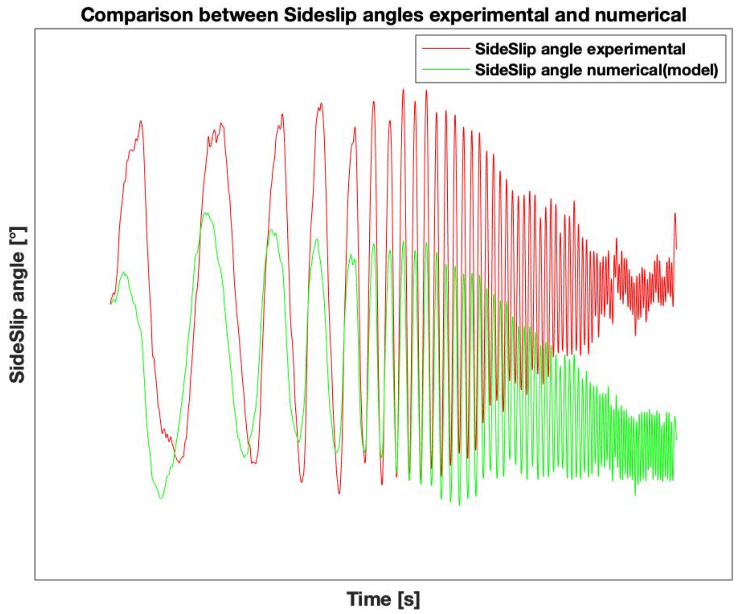

Figure 5-24 Sideslip angle estimation with Kinematic model

Using the vehicle dynamics equations for the bicycle model it is possible to obtain the estimate of the slip angles of the two axles. Clearly, for the assumptions intrinsic to the same model, errors are foreseeable.

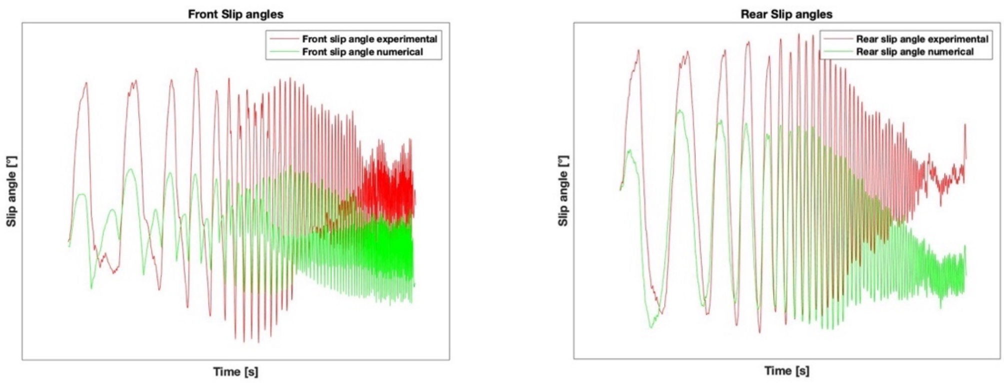

Figure 5-25 Rear and Front slip angle estimation with Kinematic model

Knowing the value of the acceleration over time and knowing the distribution of the mass of the car it is possible to obtain the distribution of the forces of the car which can be represented in Figure 5-26.

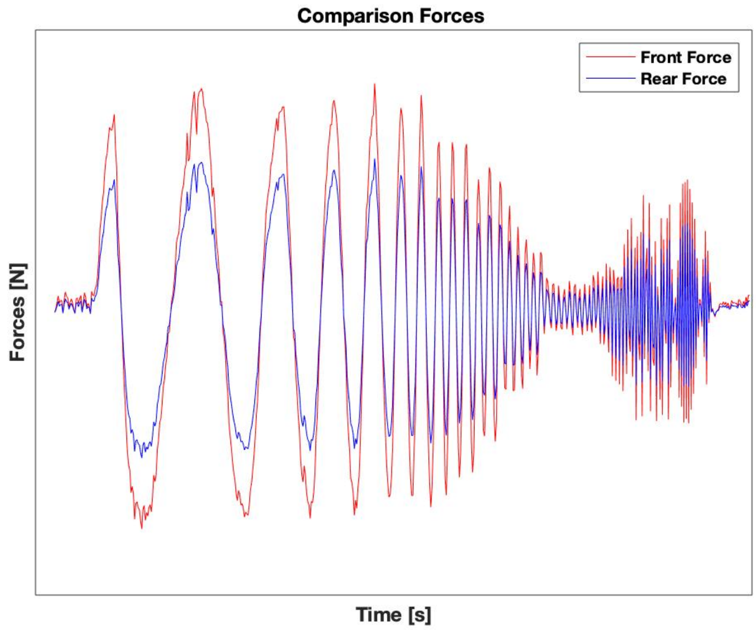

Figure 5-26 Comparison Rear and Front Forces

In the case of transient tests, and as will be seen, also for the lap tests, the procedure to be used is different from that used in the case of steady-state tests. In fact, if in the steady-state tests the cornering stiffnesses of the axles were estimated as the ratio between the lateral forces and the slip angles of the respective axle, in this case, due to the way the test is carried out, the use of this methodology is not optimal. In fact, by estimating the cornering stiffness in this way, especially in the points where there is a peak of the lateral forces, the results of the cornering stiffness are not optimal. It was therefore opted to make a steady-state pre-maneuver with that given vehicle suitably equipped, to have a first estimate of the cornering stiffness and then directly enter this data as input. Therefore, follows a flow chart that summarizes this process.

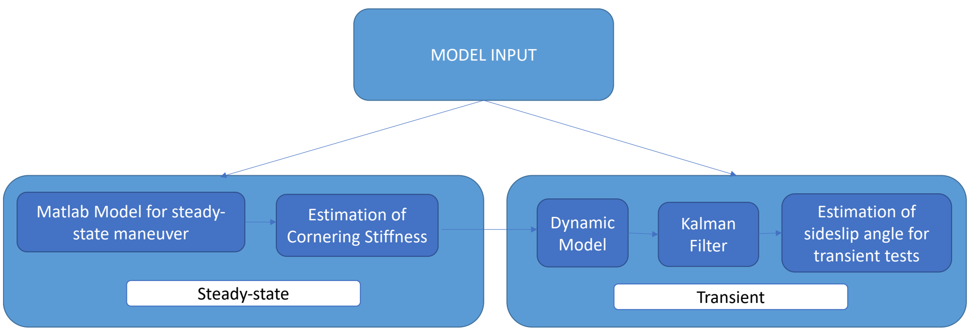

Figure 5-27 Flow chart of the Matlab model for transient test.

As can be seen from the *Figure 5-27*, the Matlab model created for the transient tests has as input, the cornering stiffnesses that are calculated by the steady-state model using a ramp steer test for that car.

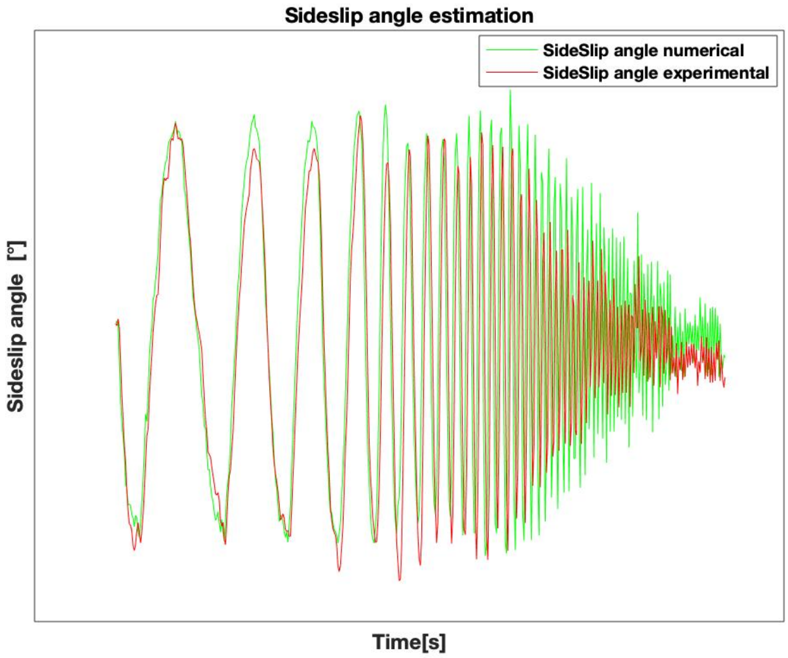

Figure 5-28 Estimation of sideslip angle with Kalman filter applicated to dynamic model

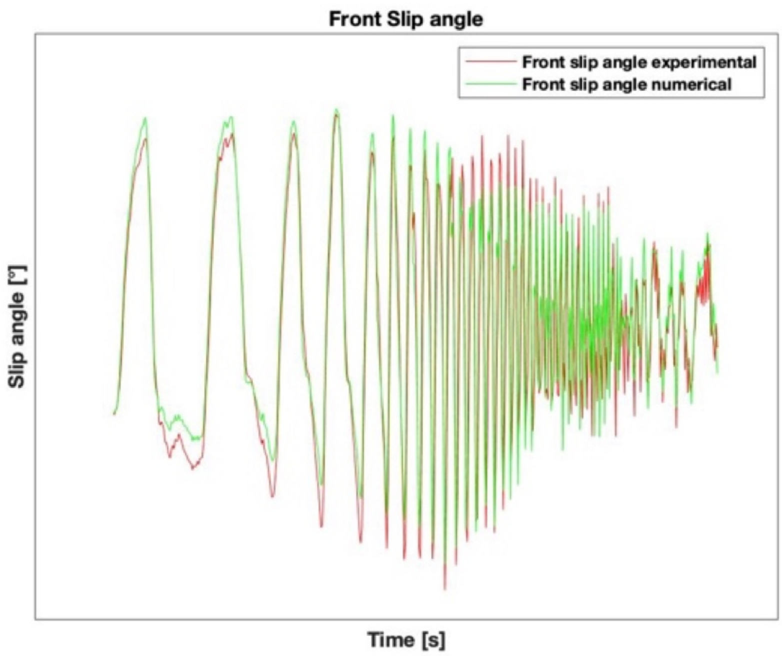

Figure 5-29 Estimation of front slip with Kalman filter applicated to dynamic model

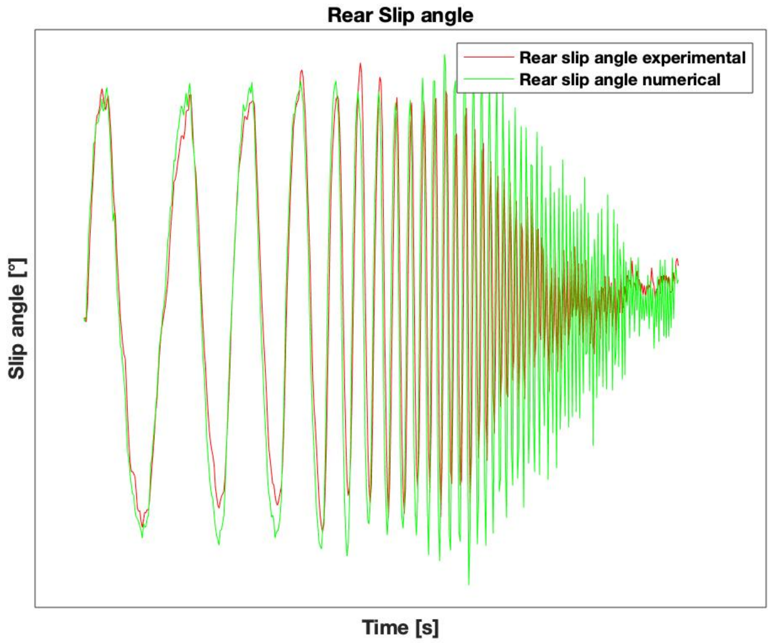

Figure 5-30 Estimation of rear slip angle with Kalman filter applicated to dynamic model

The results obtained showed a clear improvement of the sideslip angle estimate with Linear Kalman Filter. At high frequencies, however, the model overshoots the estimation. The modification of the covariance matrices and the identification of the optimum allow to achieve a better result. Also, in this case the value of Q and R has been set equal to 1e-1. Furthermore, the reliability of the same sensors at higher frequencies is lowered causing this loss of performance of the model.

In conclusion, in order to have an objective measure of the estimation error and the improvement obtained by passing from the estimation with the kinematic model only to the model that uses the Kalman filter, the parameters of MAE and RMSE errors described in paragraph 4.6 are used.

The error obtained for the above test, in terms of MAE before the application of the filter was 4.12°, while in terms of RMSE it was 4.01°. Through the application of the filter the MAE and the RMSE are drastically reduced obtaining values of 0.319° and respectively 0.454°. The *Figure 5-31* shows the trend of the error over time for the estimate of the sideslip angle.

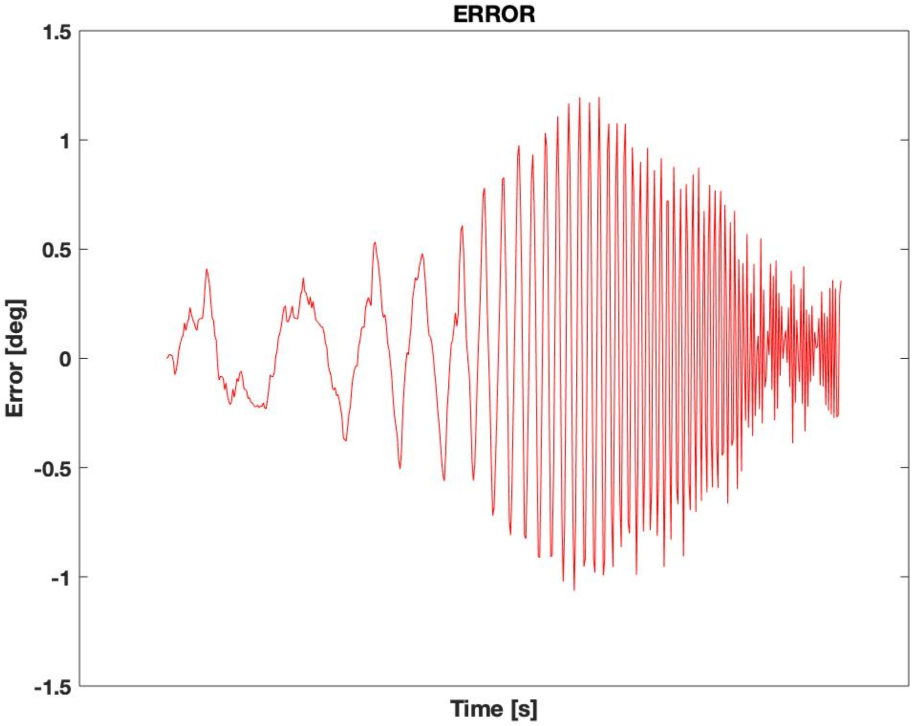

Figure 5-31 Trend of the error over time for the estimate of the sideslip angle.

5.6 Lap maneuver

The lap is a maneuver made at almost constant speed: 50 km/h, 60 km/h and 80 km/h. In this maneuver the driver should try to maintain the vehicle speed constant even in the curves, to simulate the steady state reference maneuver for several types of curves.

The Figure 5-32 show the trend of the steering wheel angle and the Figure 5-33 shows the acceleration over time for this type of maneuver.

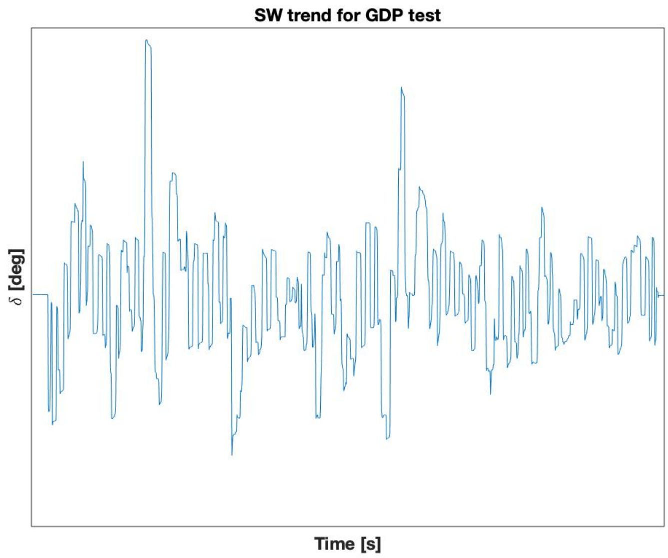

Figure 5-32 Steering wheel angle trend for GDP test

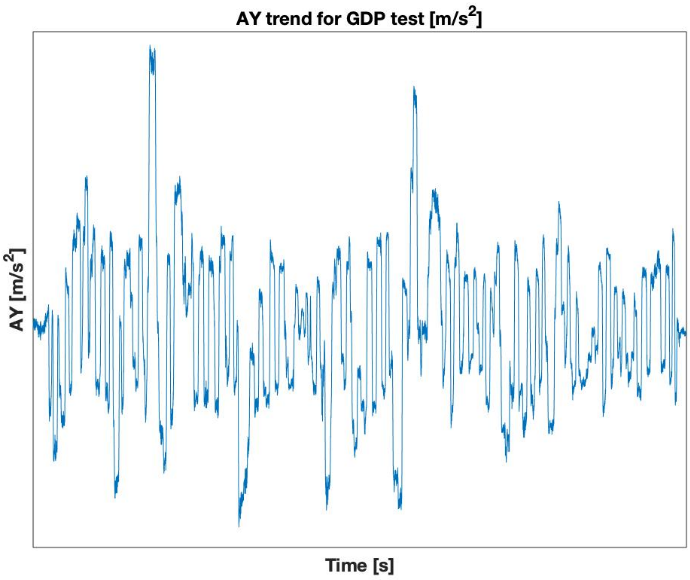

Figure 5-33 Lateral acceleration trend for GDP test

The procedure adopted also in this case is the same as seen in the previous paragraphs for transient tests. For simplicity, only the final graph for estimating the sideslip angle for the constant speed equal to 50 km/h will be plotted

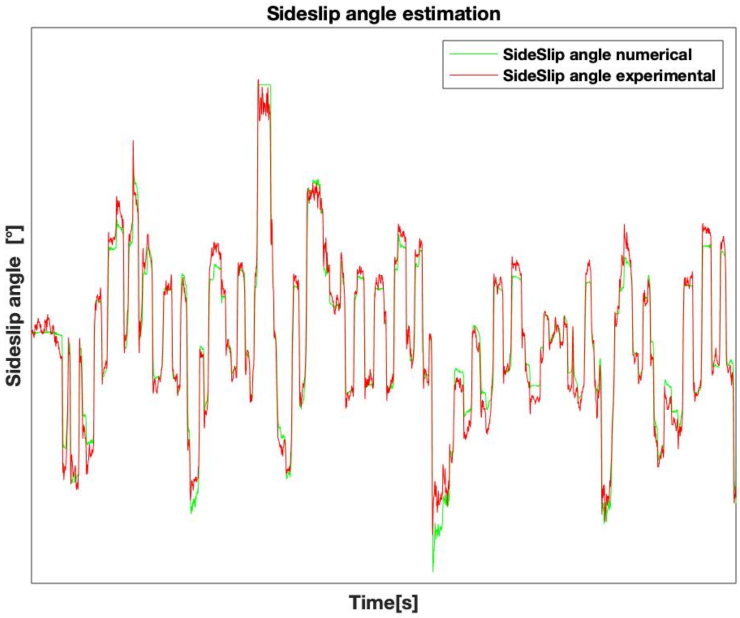

Figure 5-34 Sideslip angle estimation for lap test at 50 km/h

To better appreciate the estimation made with the model which uses the Kalman model, an enlargement of the plot in a generic interval of 10 seconds is proposed in the Figure 5-35

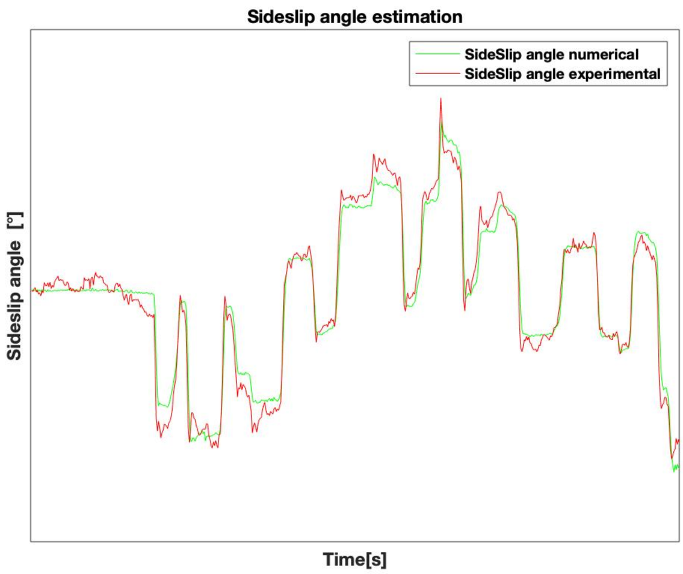

Figure 5-35 Sideslip angle estimation for an interval of 10 seconds

In order to have an objective measure of the estimation error and the improvement obtained by passing from the estimation with the kinematic model only to the model that uses the Kalman filter, the parameters of MAE and RMSE errors described in paragraph 4.6 are used.

The error obtained for the above test, in terms of MAE before the application of the filter was 4.3°, while in terms of RMSE it was 5.6 °. Through the application of the filter the MAE and the RMSE are drastically reduced obtaining values of 0.154° and respectively 0.201°.

5.7 Validation of the model for variable speed tests

The last step for the validation of the model was the analysis of the variable speed tests. As seen from the previous chapters, velocity is a vector that is introduced in the state matrices. Until now it has always been considered a constant speed.

The presence of a new variable parameter leads to an increase in terms of calculation cost and therefore we expect a higher error than what we have seen for constant speed test. So, in this case the velocity vector is a variable column vector. Therefore, having a $v_{y_{stim}}$ dependent on the vector Vel, clearly also the sideslip angle, estimated by kinematic model, obtained as the $arctg\left(\frac{v}{Vel}\right)$ is dependent on the input speed and as a consequence the cornering stiffness and the terms A, B, C, D. All these terms, therefore dependent on the velocity vector, this time variable, as seen, will be introduced in the dynamic model to which the Kalman filter is applied.

Until now through a uidget file, once the file was selected we have defined the constant speed of the vehicle. In this phase it is therefore very important to have an excellent measurement of the speed valued to the center of gravity to avoid errors in the subsequent calculation phase. Having therefore made this premise, the model continues to function as in the previous cases. Therefore, the results remain excellent as can be seen from the following figures.

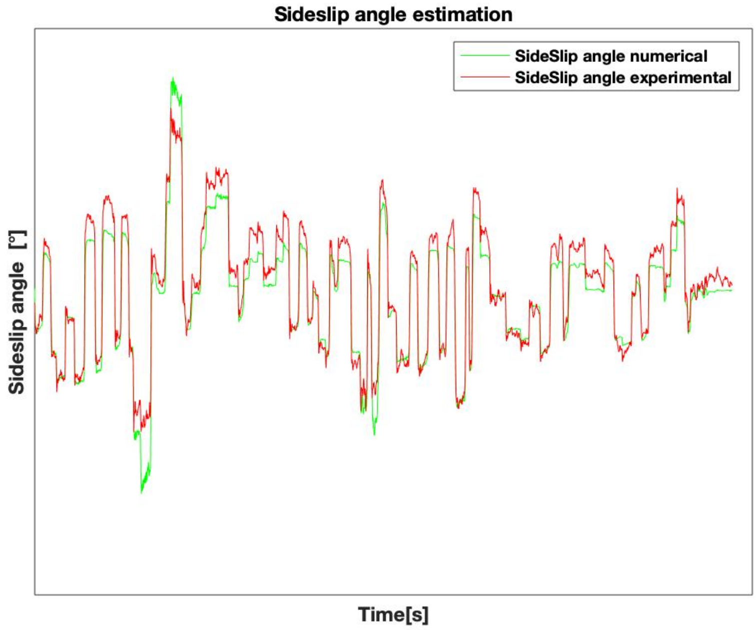

Figure 5-36 Sideslip estimation for GDP with variable velocity

From the *Figure 5-36* it is immediately visible how the average trend of the sideslip angle is well represented; however the presence of some peaks does not allow to have very low RMSE values. The model may be filtered at a lower frequency to reduce this effect. To better appreciate the trend of the sideslip angle estimation, an enlargement of the plot between 220 and 290 seconds has been plotted.

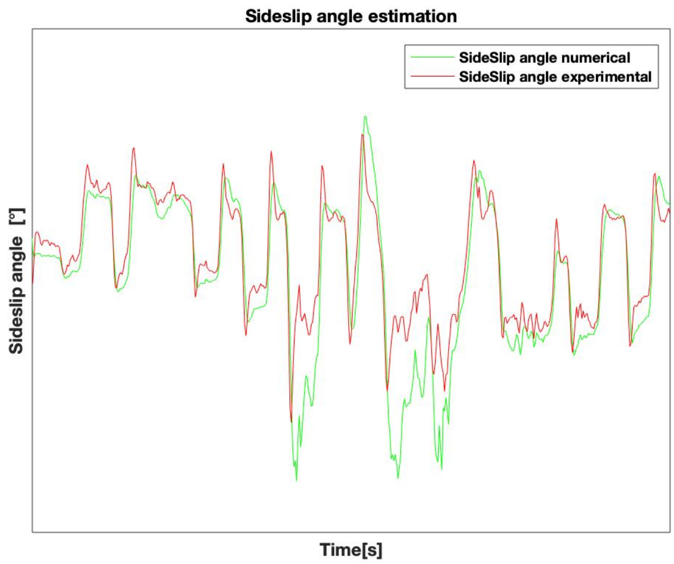

Figure 5-37 Analysis of the estimate of the sideslip angle between 220 and 290 seconds

5.8 Comparison of results

Once all the possible types of tests have been completed, a summary table is shown with the aim of summarizing what has been seen by showing the results obtained from the following generated Matlab model.

$\boldsymbol{POST - FILTER\ ERROR\ CALCULATION}^{[A]}$	
Ramp steer test (RIF. VV106DC1)	MAE è 0.142°
	RMSE è 0.183°
Sweep test (RIF. VV121F00_TH)	MAE è 0.319°
	RMSE è 0.451°
Lap test (RIF. VV050G03)	MAE è 0.201°
	RMSE è 0.350°

Table 5-3 Error calculated for different types of tests

Analyzing the results, we realize how the estimate is still very effective. Clearly, the presence of an additional variable input means that in the variable speed tests the estimation error is greater than in the other tests. Furthermore, as seen, the sweep tests concentrate the error at high frequencies where the sensitivity of the sideslip angle measurement sensor is also in question.

To increase the robustness of the model, it was validated by carrying out several tests on the same type of car but modifying the type of tires and rims. It is indeed interesting to understand if the model is able to read the difference in corning stiffness and to understand the difference with the experimental values of these provided directly by Stellantis. Therefore, 5 types of tests are defined with 5 different equipment of the same vehicle.

By following the procedure described in the previous paragraphs, it is possible to make a comparison on the estimation error of the cornering stiffness for the different equipment. Therefore, graphs will be plotted that will show the comparison between the estimate of the cornering stiffnesses obtained from the kinematic model and the real cornering stiffnesses obtained from data.

After that, graphs will be plotted showing the error between the cornering stiffness, obtained starting from the slip angle obtained from the dynamic model to which the Kalman filter is applied and making the ratio with the lateral forces, and the real cornering stiffnesses obtained from data. The results were plotted on the same scales.

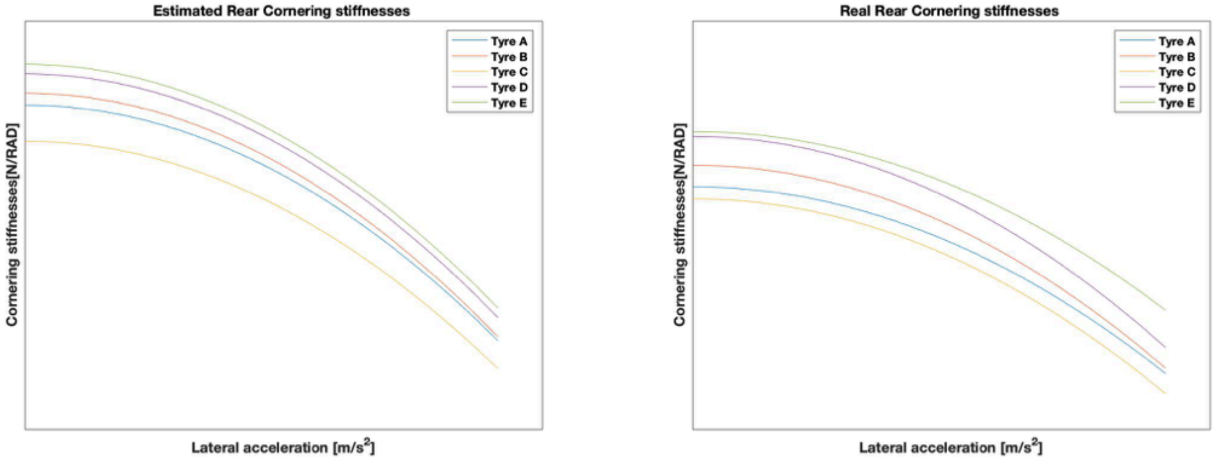

Figure 5-38 Comparison between rear cornering stiffnesses estimated by the kinematic model and real rear cornering stiffnesses for different type of tyres

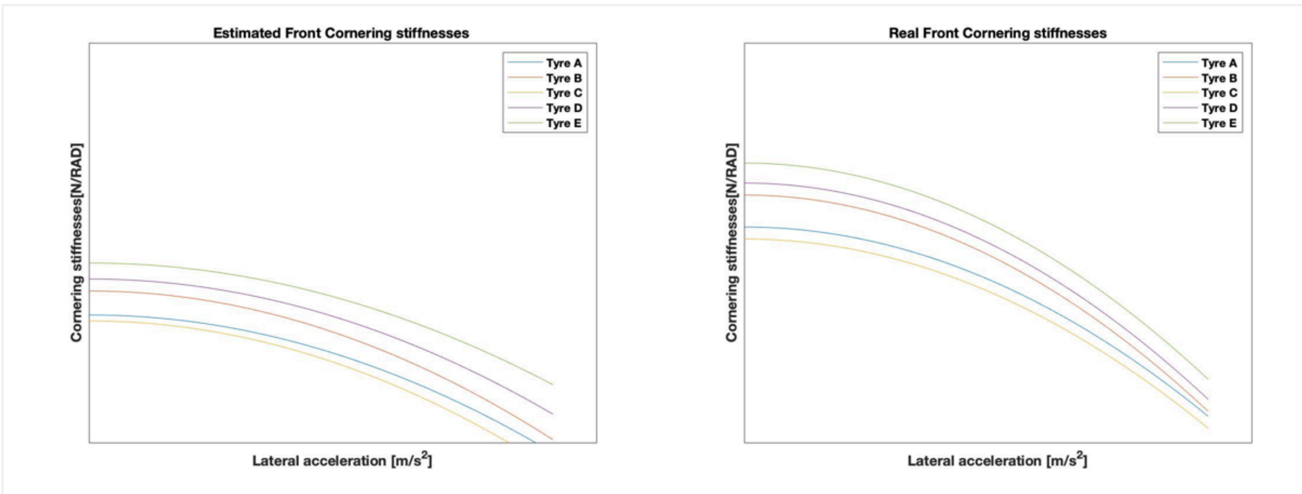

Figure 5-39 Comparison between front cornering stiffnesses estimated by the kinematic model and real front cornering stiffnesses for different type of tyres

The kinematic model is already able to evaluate the different types of tires well, however the percentage error is 15.2% for the rear stiffnesses, and 16.2% for the front ones.

It is obvious that, with the use of the dynamic model to which the Kalman filter is applied, the resulting cornering stiffnesses are more similar to the real ones. The error, in fact, in percentage decreases considerably. The *Figure 5-40* and *Figure 5-41* show the comparison cornering stiffness curves, always on the same scales.

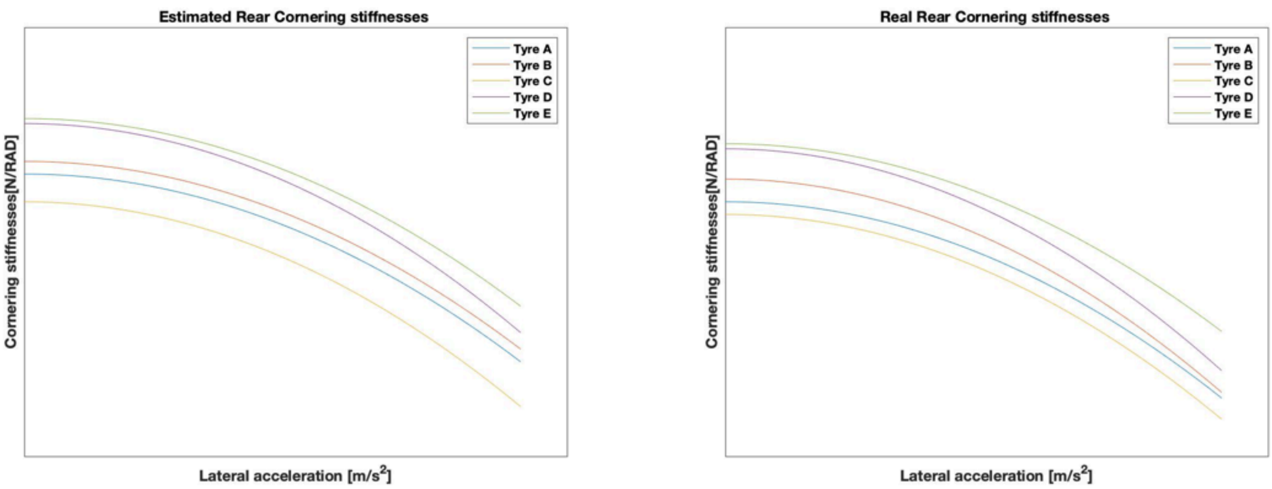

Figure 5-40 Comparison between rear cornering stiffnesses estimated by the dynamic model and real rear cornering stiffnesses for different type of tyres

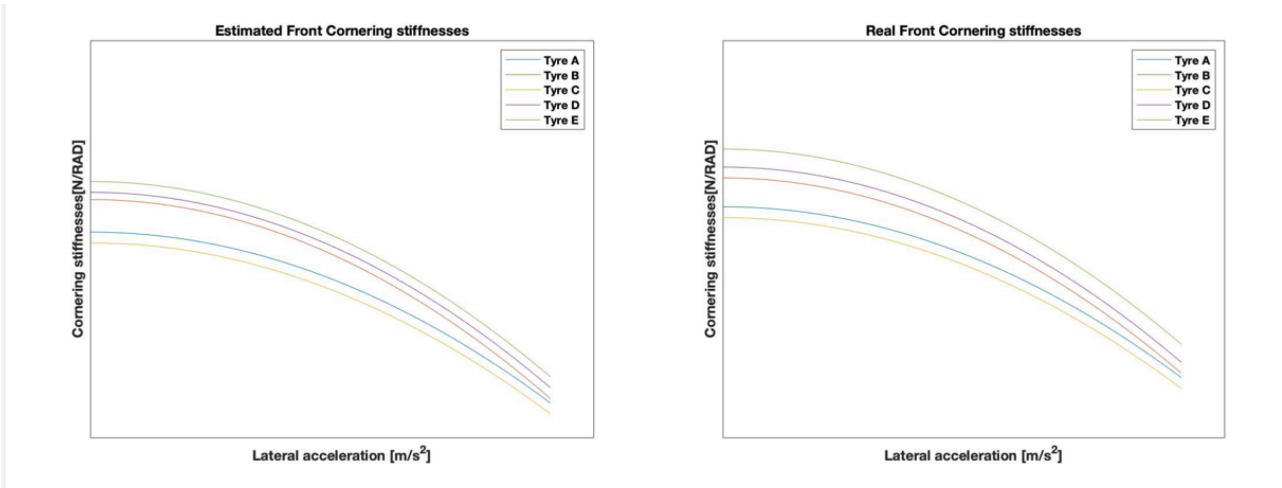

Figure 5-41 Comparison between front cornering stiffnesses estimated by the dynamic model and real front cornering stiffnesses for different type of tyres

The error in this case is 6.6% for the rear stiffnesses, while 8.2% for the front ones. These values testify, with greater objectivity, how good is the work of the Kalman filter for the model itself.

Multiple tests were performed for the same type of equipment, evaluating the error of the slip angle output and averaging it. In all, 40 ramp steer tests, 20 sweep tests and 5 runway laps were evaluated.

The results deriving from these analyzes are shown in the table:

CHI			
MAE min	0.142°	RMSE min	0.183°
MAE max	0.513°	RMSE max	0.561°
MAE (average)	0.282°	RMSE (average)	0.330°

Table 5-4 Results for CHI (ramp steer) tests.

SWEEP			
MAE min	0.243°	RMSE min	0.333°
MAE max	0.357°	RMSE max	0.466°
MAE (average)	0.310°	RMSE (average)	0.405°

Table 5-5 Results for SWEEP tests.

LAP			
MAE min	0.171°	RMSE min	0.222°
MAE max	0.261°	RMSE max	0.569°
MAE (average)	0.22°	RMSE (average)	0.381°

Table 5-6 Results for LAP tests.

It can be seen that the lowest values of the tests are obtained for the LAP tests. Nevertheless, the best average values were obtained for the LAPs. The reason is that, having tested the model for 40 ramp steer tests, some of them could have been performed in a bad way, therefore it would be necessary, before starting the model, to make a pre-screening of the tests, in this sense the results that are they would get would be even better than those shown in the tables above.

The sweep tests, as expected, show the biggest errors, being in fact transient tests the model has more difficulty in predicting the sideslip angle of the car. Therefore, especially at high frequencies, there is an overshoot that proves a greater error than the ramp steer and lap tests.

A further analysis that has been carried out is the comparison between the understeer curves estimated by the model and the real ones. The experimental curve was provided directly from Stellantis internal files. With reference to the tests with type A tires, it is important to make a comparison of the understeer curves, evaluating the values at fixed accelerations. The errors obtained for example with lateral acceleration equal to 0.4g is 9.8% against an error of 7.7% for the lateral acceleration of 0.7g.

Chapter 6

6. Conclusion and Outlook

Recent developments in the automotive field are focused on making the car more efficient and safer. From this point of view, the sideslip angle of a vehicle plays a key role in terms of driver safety.

Currently, the measurement of the sideslip angle of a vehicle during a test is entrusted to an optical sensor which is very expensive and not normally present on cars.

The aim of the following thesis project is to obtain the sideslip angle of the vehicle without using an optical sensor but relying only on the data provided by the inertial platform or the CAN network and the steering torque sensor. The model is based on the principles of lateral dynamics of a vehicle. In particular, the bicycle model was studied in depth, which turns out to be an excellent compromise between simplicity and results obtained.

To calculate the sideslip angle using the model it is necessary, after obtaining the measurements from the respective sensors, to calculate the slip angles of the two axles using the kinematic model with which it is possible to estimate the cornering stiffness that is introduced inside the dynamic model of the vehicle to which the Kalman filter is applied. Among the different types of recursive filters, a linear Kalman filter was chosen given the nature of the equations involved and for the target of obtaining a model that would provide results in a very short time but, at same time, had the lowest possible computational cost. The filter is based on the covariance matrices Q and R, which have been set after the considerations seen in the previous chapters in order to obtain valid results for all tests.

To validate the model, different types of tests were performed (steady state, transient or tests that included stationary parts and transient parts) with different types of cars or with the same car but modifying the type of tyre and rim. The model alone is able to define the start and end of the test and to return sideslip angle values close to the real ones and to detect the different cornering stiffnesses based on the type of tire equipped on the car. The error obtained, both in terms of MAE and RMSE, is clearly lower for stationary tests, while higher for transient or variable speed ones.

The model is based on the simplifications induced by the bicycle model and it would be interesting to deepen the discussion using more complicated models that included longitudinal dynamics as well as lateral dynamics.

In conclusion, the model generated is a model capable of providing a good estimate of the sideslip angle of the car during the test, and still working on the model by complicating and improving it and hopefully reducing the error again, one might even think to replace the optical sensor with the above model. This allows car companies to save a lot of money.

As future developments of the model it is certainly necessary to include within it the part related to the relaxation length using a Kalman filter with four states rather than two. This with the aim of significantly improving the results obtained especially for the transient and random tests. It would also be interesting to evaluate the cost-benefit relationship obtained using more complicated vehicle dynamics models than those used in the following algorithm.

Bibliography

[1] Zhanglin Cai, Stephen Chan, Xiaofeng Tang and Jiang Xin, The Process of

Vehicle Dynamics Development.

[2] Thomas D.Gillespie, Fundamentals of Vehicle Dynamics, SAE International, 1992.

[3] Giancarlo Genta, Lorenzo Morello, L'AUTOTELAIO VOL. 2, PROGETTO DEI SISTEMI, Levrotto & Bella, 2007.

[4] Course notes of "Impostazione Progettuale dell'Autoveicolo", Enrico Galvagno

[5] Daniel Chindamo, Basilio Lenzo, and Marco Gadola. «On the vehicle sideslip angle estimation: a literature review of methods, models, and innovations». In: *applied sciences* 8.3 (2018), p. 355 (cit. on pp. 2, 3).

[6] B.L. Boada, M.J.L. Boada, V. Díaz (2016). Vehicle sideslip angle measurement based on sensor data fusion using an integrated ANFIS and an Unscented Kalman Filter algorithm. *Mechanical Systems and Signal Processing*, 72-73. Pp. 832–845.

[7] Enrico Galvagno, Mauro Velardocchia. Meccanica del veicolo Esercitazioni 2010, CLUT pp. 42-46

[8] Mingyuan Bian, Long Chen, Yugong Luo, and Keqiang Li. A Dynamic Model for Tire/Road Friction Estimation under Combined Longitudinal/Lateral Slip Situation, Conference Paper in SAE Technical Papers · April 2014

[9] S. Konatowski & A. T. Pieniężny ,A comparison of estimation accuracy by the use of KF, EKF & UKF filters Conference: CMEM June 2007

[10] Ramsey Faragher, Understanding the Basis of the Kalman Filter Via a Simple and Intuitive Derivation, IEEE SIGNAL PROCESSING MAGAZINE [129-131] SEPTEMBER 2012

[11] Furqan Asghar Muhammad Talha In-Ho Ra Sung Ho Kim, Simulation study on battery state of charge estimation using Kalman Filter Article November 2016

[12] Pieter Blok, K. Van Boheemen, Robot navigation in orchards with localization based on Particle filter and Kalman filter, Article February 2019

[13] Valeria Mangiapane Sensor fusion mediante filtro Bayesiano (Kalman Filter), 2016

[14] Rolfo Gian Luca, Comparison between optical and GPS systems for sideslip angle measurements

[15] Dan Simon, Optical State Estimation, Cleveland State Univeristy, John Willey &Sons 2006, pp71, 107-111.

[16] T.Kailath,A.Sayed,andB.Hassibi,*LinearEstimation,*Prentice-Hall, Upper Saddle River, New Jersey, 2000.

[17] P. Stein, “Some general theorems on iterants,” Journal of Research of the National Bureau of Standards, 48, pp. 82-82 (1952).

[18] Rizzoni et al, Proceedings of the 44th IEEE Conference on Decision and Control, and the European Control Conference 2005 Seville, Spain, December 12-15, 2005

[19] Notes of “Control of pollutant emissions”

[20] Phillip F. Schewe, Complex hybrid structures, 01 APRIL 2005

[21] M. Ehsani, Modern Electric, Hybrid Electric and Fuel Cell Vehicles: Fundamentals, Theory and Design, CRC Press, 2005

[23]Pierdomenico Ruggieri Studio del modello CDTire per analisi Handling e Ride Comfort di un veicolo in relazione ai parametri geometrici e operativi degli pneumatici

Sitography

[24] https://en.wikipedia.org/wiki/Fuzzy_logic

[25] http://racingcardynamics.com/racing-tires-lateral-force/

[26] https://en.wikipedia.org/wiki/Kalman_filter

[27] https://en.wikipedia.org/wiki/Understeer_and_oversteer

[28] https://en.wikipedia.org/wiki/Hybrid_electric_vehicle

Appendix A

Type of Test	
Ramp steer test (CHI) **(RIF. VV106DC1)**	VV106= test with speed of 100 km/h and duration of 6 seconds DC=Ramp steer to the right; SC=Ramp steer to the left; 0,1,2 = test reference number
Sweep test **(RIF. VV121F00_TH)**	VV121=Test with speed of 120 km/h 1=index for lateral acceleration, for example 1 = 0.3 g; 2=0.6g F= Sweep Test 0,1,2= test reference number
Lap test **(RIF. VV050G00)**	VV050=Test with speed of 50km/h G= lap of the track 0,1,2= test reference number